Construction and Building Materials 123 (2016) 673–689

Contents lists available at ScienceDirect

Construction and Building Materials

journal homepage: www.elsevier.com/locate/conbuildmat

Review

Recycling combustion ash for sustainable cement production: A critical review with data-mining and time-series predictive models

Yu Wang [a], Yixin Shao [b], Miodrag Darko Matovic [c], Joann K. Whalen [d,*]

[a] School of Computer Science, Georgia Institute of Technology, Atlanta, GA 30332, United States
[b] Department of Civil Engineering, McGill University, Montreal, Quebec H3A 0C3, Canada
[c] Department of Mechanical and Materials Engineering, Queen's University Kingston, Ontario K7L 3N6, Canada
[d] Department of Natural Resource Sciences, Macdonald Campus of McGill University, 21111 Lakeshore Road, Ste-Anne-de-Bellevue, Quebec H9X 3V9, Canada

HIGHLIGHTS

- Critically reviewed the recent research progress on various ashes as pozzolans.
- Created data-mining artificial neural network to predicting pozzolanic activity.
- Quantified the effect of cement curing on pozzolans by a time-series model.
- Accurately forecast the pozzolanic activity in 3–90 d curing (R^2 = 0.8479–0.9914).
- Recommended this model as a rapid estimator of pozzolanic activity before testing.

GRAPHICAL ABSTRACT

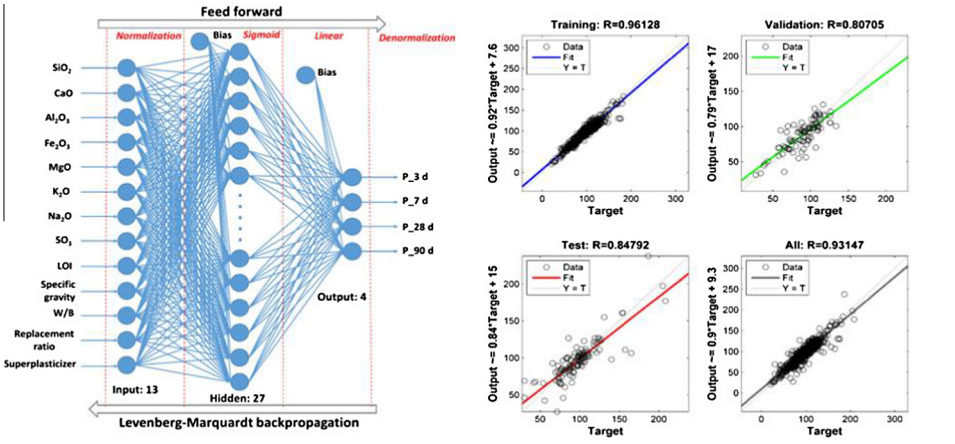

ARTICLE INFO

Article history:
Received 23 February 2016
Received in revised form 3 July 2016
Accepted 12 July 2016

Keywords:
Combustion ash
Cement production
Waste recycling
Artificial neural network
Time-series analysis

ABSTRACT

Combustion is a complex process that produces energy as the goal and ashes as by-products. The ash of coal, biomass and solid waste combustion can be used as pozzolans in blended cement due to the similarity of their physiochemical properties to conventional pozzolans (e.g. silica fume). This strategy effectively recycles pozzolanic-active combustion ash and replaces a significant proportion of Portland cement, which potentially reduces the greenhouse gas (GHG) emissions from cement production. However, cement producers wishing to substitute pozzolanic-active ash for conventional pozzolans lack information on the pozzolanic activity (PA) of ash from diverse combustible materials. A data-mining model that can extract key information for predicting the PA of combustion ash is envisioned as a screening tool to assess the pozzolanic potential of candidate combustible materials prior to experimental work. Hence, the objectives of this chapter are, 1) to critically review the recent research progress in using various combustion ashes as pozzolans, including the mechanism of the pozzolanic reaction, sources of eligible materials, and methods of PA improvement, 2) to create a data-mining artificial neural network (ANN) model for PA prediction built upon data reported in the scientific literature from 1998 to 2015, and 3) to describe the effect of cement curing period on PA, based on a time-series model. The ANN and time-series models developed in this study can accurately forecast

* Corresponding author.
E-mail address: joann.whalen@mcgill.ca (J.K. Whalen).

http://dx.doi.org/10.1016/j.conbuildmat.2016.07.031

the PA of combustion ashes during 3–90 d curing (R^2 = 0.8479–0.9914). We recommend these screening tools as rapid indicators of the pozzolanic potential of combustion ash prior to undertaking strength tests and other experimental testing.

Contents

1. Introduction

The Portland cement industry relies upon the pozzolanic reaction to achieve the desired binding and structural strength in cement products at a lower economic cost than using Portland cement alone. A pozzolan is a siliceous or siliceous-aluminous material with virtually no cementitious function. In the presence of water, it reacts with $Ca(OH)_2$, hereafter referred to as CH, to generate $(CaO)_x{\cdot}(SiO_2)_y{\cdot}(H_2O)_z$, the C-S-H complex that is the key contributor to concrete strength [22,84]. Supplemental C-S-H formation during cement hydration due to the pozzolanic reaction can improve concrete properties such as strength and durability [132]. Yet, the cement—pozzolan—water mixture is a complex system, consisting of many physicochemical processes that are influenced by temperature, mixing proportion, pozzolan reactivity, pozzolan particle size and other factors. The challenge is to choose a suitable and economically feasible pozzolan with the right physicochemical characteristics to assure the final quality of concrete.

Up to 50% of the Portland cement can be replaced by a pozzolan in a blended cement without any adverse impact on concrete performance [50,71]. Blending cement with silica-rich pozzolans like volcanic ash, diatomaceous earth and silica fume is a practice dating back to antiquity, based on structures built more than 2000 years ago by Greek and Roman civilizations [67]. Solid wastes such as combustion ash and catalyst residue can be used as a pozzolan if they possess physiochemical properties akin to conventional pozzolans (e.g. silica fume). An eligible pozzolan should be rich in siliceous or siliceous-aluminous compounds and have a fine particle size (<45 μm) [114]. This strategy effectively recycles these pozzolanic-active resources and reduces the amount of Portland cement needed to make strong and durable concrete, which potentially reduces the greenhouse gas (GHG) emissions from cement production [61,66]. Considering these environmental benefits in the context of sustainable cement production, many researchers have tested the pozzolanic activity (PA) of various solid wastes and reported their findings in the scientific literature, leading to more than 1612 publications on this topic in the Web of Science from 2005 to 2014. On the other hand, there are few papers that synthesize, critically analyze and discuss the findings to date. If solid wastes could be recycled as pozzolans without adverse impact on cement properties, these abundant wastes that costs little or nothing can lessen the demand for Portland cement, thus helping cement industry reduce its greenhouse gas (GHG) emissions. Therefore, a review study is indispensable to comprehensively understand the potential for recycling of solid waste as pozzolan.

The sizable database of experimental studies that evaluated the pozzolanic activity (PA) of diverse solid wastes can be used to develop a data-mining model that predicts the PA of these materials. The advantage of a data-mining model is that trends can be analyzed and generalizations made, giving the cement industry a robust screening tool to assess the pozzolanic potential of a waste material before undertaking experimental work. An artificial neural network (ANN) is an appropriate predictive tool for this purpose because ANN is a high-level data-mining algorithm that simulates

the learning behavior of human neurons to mathematically address complicated and nonlinear objectives [32,155]. Using an ANN model, Pala et al. [93] and Topcu and Sarıdemir [133] successfully predicted the PA of fly ash, and noted minor deviation between predicted and experimental results ($R^2 > 0.8$). Predictive ANN models of PA in combustion ashes were described by Prasad et al. [107], Atici [9], Dantas et al. [35], and Duan et al. [37] for proving the modeling applicability. Although these studies show the potential of ANN models for PA evaluation, they have limited relevance to the cement industry because each study considered a single pozzolan and relied on small datasets (<100 groups of experimental results) derived from their own experimental results or a subset of values for a particular pozzolan from the scientific literature. Thus, the published ANN models do not consider the PA of diverse solid wastes that could potentially be pozzolans in cement production. Another major limitation of the published ANN models is that they do not consider pozzolan reaction time explicitly, although, time has a crucial role in the development of chemical bonds and physical structure in the cement—pozzolan—water system [122]. Hence, an enhanced ANN model is needed to build on the existing knowledge and to extend analysis to a broader dataset that describes the many pozzolanic materials that may be considered by the cement industry. In addition, since the curing age reflects the pozzolan reactivity during cement hydration, the predictive model must also include a time-series function that reveals the correlation between curing age and PA in blended cement.

Therefore, the objectives of this paper are to, 1) systematically review the literature on using solid wastes as a pozzolan, including the mechanism of pozzolanic reaction, sources of eligible materials, and methods of PA improvement, 2) create an enhanced ANN model to predict PA in blended cement that includes 22 solid wastes that are potential pozzolanic materials, and 3) evaluate the effect of curing age on PA in blended cement based on a time-series model.

2. Mechanism of pozzolanic reaction

As the pozzolanic reaction is highly associated with cement hydration, we begin by describing the principle of cement hydration. Portland cement typically contains four cementitious components, including 45–75% tricalcium silicate ($(CaO)_3{\cdot}SiO_2$, abbreviated as C_3S), 7–32% dicalcium silicate ($(CaO)_2{\cdot}SiO_2$, C_2S), 0–13% tricalcium aluminate ($(CaO)_3{\cdot}Al_2O_3$, C_3A), and 0–18% tetracalcium aluminoferrite ($(CaO)_4{\cdot}Al_2O_3{\cdot}Fe_2O_3$, C_4AF) [17]. When these compounds interact with water, major cement hydration occurs by the following reactions (Eq. (1)–(4)):

$$(CaO)_3 \cdot SiO_2 + H_2O \rightarrow (CaO)_x \cdot (SiO_2)_y \cdot (H_2O)_z + Ca(OH)_2 \quad (1)$$

$$(CaO)_2 \cdot SiO_2 + H_2O \rightarrow (CaO)_x \cdot (SiO_2)_y \cdot (H_2O)_z + Ca(OH)_2 \quad (2)$$

$$(CaO)_3 \cdot Al_2O_3 + H_2O \rightarrow (CaO)_x \cdot (Al_2O_3)_y \cdot (H_2O)_z \quad (3)$$

$$(CaO)_4 \cdot Al_2O_3 \cdot Fe_2O_3 + H_2O \rightarrow (CaO)_x \cdot (Al_2O_3)_y \cdot (Fe_2O_3)_z \cdot (H_2O)_w \quad (4)$$

where the $(CaO)_x{\cdot}(SiO_2)_y{\cdot}(H_2O)_z$, (C-S-H) complex is the key hydration product that contributes to the strength of cementitious products, e.g. concrete [110]. It should be noted that SO_4^{2-} and CO_2 may also participate in the major cement hydration reactions, and interact with the reactions above, such as through the carbonation process. C_2S is hydrated more slowly than C_3S, so the early and late strength measured during curing benefit from C_3S and C_2S hydration, respectively. Conversely, the strength conferred by C_3A and C_4AF hydration is trivial, since their hydrated products $(CaO)_x{\cdot}(Al_2O_3)_y{\cdot}(H_2O)_z$, hereafter designated as C-A-H and $(CaO)_x{\cdot}(Al_2O_3)_y{\cdot}(Fe_2O_3)_z{\cdot}(H_2O)_w$ known as C-A-F-H, are microstructurally weaker than C-S-H [72]. Hence, the hydration of C_3S and C_2S will release Ca^{2+} ions, which dissolve rapidly from solid C_3S and C_2S when cement is mixed with water, leading to a supersaturated Ca^{2+} concentration in the cement-water slurry. With excess Ca^{2+}, the C-S-H gel forms swiftly along with the crystallization of CH. This process is controlled by ionic diffusion through the porous structure formed by C-S-H and tends to decrease with time owing to the diminution of capillary porosity, which slows the hydration rate steadily during the curing period [152]. Crystalline CH inhibits the directional growth of C-S-H crystal, making the concrete susceptible to failure if a force is applied across the C-S-H crystal plane. Therefore, lowering the proportion of CH present during cement hydration might be an option to improve the strength and durability of concrete.

The pozzolanic reaction is one way to reduce the CH contained in cement because it can transforms CH into other compounds that contribute to concrete strength [42]. When a pozzolan is added during the cement hydration phase, the surface of the pozzolan is attacked by dissolved OH^-, thus forming a thin film around the pozzolan particle. As CH dissolution is reversible, the concentrations of Ca^{2+} and OH^- increase quickly, which stimulates the dissolution of SiO_2, Al_2O_3 and Fe_2O_3 from the pozzolan (Eq. (5)-(7)) [124].

$$Ca(OH)_2 + SiO_2 \rightarrow (CaO)_x \cdot (SiO_2)_y \cdot (H_2O)_z \quad (5)$$

$$Ca(OH)_2 + Al_2O_3 + H_2O \rightarrow (CaO)_x \cdot (Al_2O_3)_y \cdot (H_2O)_z \quad (6)$$

$$Ca(OH)_2 + Al_2O_3 + Fe_2O_3 + H_2O \rightarrow (CaO)_x \cdot (Al_2O_3)_y \cdot (Fe_2O_3)_z \cdot (H_2O)_w \quad (7)$$

Extra C-S-H, C-A-H and C-A-F-H are produced by the transformations described above, which promotes the strength and durability of concrete [64]. These reactions generally commence one or more weeks after the start of cement hydration. This delay is ascribed to the dependency of the pozzolanic reaction on the formation of crystallized CH, and the evolution of the pH to a level that permits dissolution of pozzolanic compounds. Despite these descriptions, this cement—pozzolan—water system is still not yet wholly understood, since numerous, interdependent physiochemical changes take place during this process.

Microscopic evaluation of the pozzolanic reaction in cement—pozzolan—water system reveal physical modifications of the cement microstructure when silica fume [13,130,135,146,152] and low-calcium fly ash [145] are selected as pozzolans. Besides promoting C-S-H formation, finely ground pozzolans act as physical fillers, which reduces the pore size and blocks capillary pores of the C-S-H gel, thus making the concrete denser [52]. Experimentally, the cement-pozzolan-water mixture exhibited a delay (normally >10 h) in the pozzolanic reaction that made concrete more permeable at early curing age (owing to the lower proportion of Portland cement), and then the concrete would become more compact [135]. Once curing was complete, the lower permeability and denser structure of the cement-pozzolan-water mixture augmented the concrete durability, conferring greater resistance to the sulfate attack, efflorescence, shrinkage, thermal cracking, chlorine corrosion, and alkali silica reaction (ASR) expansion than Portland cement-water mixtures [82]. In summary, these microscopic studies attest that the physicochemical properties of pozzolans are effective in making concrete stronger and more durable.

3. Sources of the eligible solid wastes as pozzolans

3.1. Eligibility of pozzolanic materials

In view of the requirements of the pozzolanic reaction, a qualified pozzolan should contain an adequate content of amorphous SiO_2, Al_2O_3 and Fe_2O_3 to assure its chemical reactivity. Second, its particle size should be fine enough to guarantee the sufficiently large reactive surface area for the pozzolanic reaction [80]. At present, there are two internationally recognized standards to define the eligibility of pozzolans, including ASTM C618 [6] and EN 196 [16]. ASTM C618 is the reference standard in North America, which indicates that an acceptable pozzolan should have at least 70% $SiO_2 + Al_2O_3 + Fe_2O_3$, and no more than 34% of particles are retained on a 45 μm sieve (No. 325) (Table 1). Although ASTM C618 was developed to describe the minimum criteria for coal fly ash as a pozzolan, this standard was applied to other pozzolans such as biomass ash. For example, Wang et al. [144] argued that ASTM C618 should be expanded to include biomass fly ash as pozzolan, since concrete properties were not be affected by mixtures containing 25% of herbaceous and wood ash with Portland cement. This argument was also supported by Wang and Baxter [143] following a complete investigated of the impact of biomass fly ash on concrete strength, microscopic structure and durability. However, ASTM C618 does not control the water-binder ratio (W/B) during the concrete preparation. For this reason, Pourkhorshidi et al. [106] questioned the rationality of ASTM C618 compared to EN 196, since pozzolans (Trass, Tuff and Pumice) with a high PA according to ASTM C618 did not consistently improve the strength and durability of concrete, but the pozzolanic classification made by EN 196 agreed well with experimental results. An alternative, unbiased method to define the eligibility of pozzolans was developed by Vassilev and Vassileva [138], who relied on the amorphous (glassy) content in ash crystal to classify as high PA (82–100% of glass), medium PA (65–82%) and low PA (30–65%). The authors indicate that their method could simply and precisely estimate the PA of ash by testing its mineral-phase composition (quartz, mullite, sulfates, oxyhydroxides and glass).

Regardless of the method used to evaluate potential pozzolans, any candidate material should have high PA, which implies a high amount of amorphous $SiO_2 + Al_2O_3 + Fe_2O_3$ and small particle size. Many solid wastes meet these requirements, and our literature review found more than 158 reports of PA in solid wastes with variable pozzolanic functions related to their different physio-chemical characteristics (Table 2). Still, some general trends can be discerned according to the origin of these materials, and we focus on the following categories: combustion ashes, blast furnace slags, and other solid wastes.

Table 1
Chemical and physical criteria that qualify coal fly ash as a pozzolan according to ASTM C618 [6].

ASTM C618 criteria	Class N (Natural pozzolan)	Class F	Class C
Chemical requirement			
$SiO_2 + Al_2O_3 + Fe_2O_3$, min, %	70	70	50
SO_3, max, %	4	5	5
Moisture content, max, %	3	3	3
Loss on Ignition (LOI), max, %	10	6	6
Physical requirement			
Amount retained when wet-sieved on 45 μm (No. 325) sieve, max, %	34	34	34
Strength with Portland cement, at 7 d, min, % of control	75	75	75
Strength with Portland cement, at 28 d, min, % of control	75	75	75
Water requirement, max, % of control	115	105	105
Autoclave expansion or contraction, max, %	0.8	0.8	0.8

3.2. Combustion ashes

3.2.1. Coal fly ash

The fly ash from coal combustion is the most common solid waste used as a pozzolan. Fly ash is captured by bag-houses or electrostatic precipitators and removed from exhaust flue before it exits the chimney of a coal-fired power plant. It is normally light tan in color and consists mostly of silt-sized and clay-sized glassy spheres [15]. Since this ash is often rich in $SiO_2 + Al_2O_3 + Fe_2O_3$, it has potential to be recycled as a pozzolan [69]. Based on its chemical properties, fly ash is categorized as a Class F or Class C pozzolan by ASTM C618 (Table 1). Class F fly ash from anthracite or bituminous coal combustion is expected to have $\geqslant$70% $SiO_2 + Al_2O_3 + Fe_2O_3$. In contrast, Class C fly ash from lignite or subbituminous coal combustion has 50–70% $SiO_2 + Al_2O_3 + Fe_2O_3$ content. It might contain $\geqslant$10% CaO, thus also possessing cementitious properties in addition to its pozzolanic function [6]. Consequently, the PA of class F and class C fly ashes have been studied extensively.

Class F fly ash is an acceptable pozzolan in blended cement. For instance, fly ash with 86.3% $SiO_2 + Al_2O_3 + Fe_2O_3$ content could be substituted for up to 50% cement without any negative impact on concrete strength [126]. Mixing this ash in cement before casting further improved the properties of concrete (strength and abrasive resistance) continuously after 91 d or 365 d curing. However, the concrete made from blended cement was weaker than that from Portland cement in the early stage of curing ($\leqslant$28 d) due to a delay in the pozzolanic reaction during the early cement hydration period. This implies that a longer curing period may be required for blended cement with fly ash to achieve similar strength as Portland cement. Still, another Class F fly ash (96.6% $SiO_2 + Al_2O_3 + Fe_2O_3$) lessened the micro-cracking width of concrete from 4.80 μm to 3.73 μm, since it increased the Si proportion in concrete from 1.67 Si/Ca ratio to 2.09 Si/Ca ratio [55]. In addition to regular strength and structure analyses, Lorenzo et al. [79] assessed the performance of a Class F fly ash (82.3% $SiO_2 + Al_2O_3 + Fe_2O_3$) in a simulated marine environment (0.03 mol/L $Na2SO_4$ + 0.45 mol/L NaCl) and found that replacing 35% cement by fly ash raised the corrosion resistance of concrete by nearly two-fold. The diffusion of SO_4^{2+}, Na^+ and Cl^- under experimental conditions activated the ash reactivity of ash, thus making the microstructure of concrete more compact and durable.

Despite having lower $SiO_2 + Al_2O_3 + Fe_2O_3$ content, Class C fly ash is a qualified pozzolan in cement mixtures. Nassar et al. [89] assessed the practicality of blending a Class C fly ash with cement during large-scale road construction, finding that the concrete road base with 25% fly ash showed better strength (≈36 MPa) and abrasive resistance (≈0.31 mg mass loss) than concrete made from Portland cement alone (≈32 MPa and ≈0.35 mg). These advantages were attributed to the pozzolanic reaction of the fly ash, which made the microstructure of cement paste stronger and more compact. Nassar et al. [89] concluded that the fly ash pozzolan can reduce the demand for cement, thus making the capital cost of construction more economical while guaranteeing the service life and quality of infrastructure.

Coal-fired power plants generate another agglomerated ash that is not carried by exhaust gas, termed bottom ash [18,76]. It falls to the bottom of the combustion unit because it has larger particle size than fly ash or because it adheres to the hot side walls of boiler. Bottom ash is gray to black in color, and it is normally coarser (35.0 μm) than fly ash (13.9 μm) [26,97]. Yet, bottom ash has chemical properties akin to Class F fly ash, being rich in $SiO_2 + Al_2O_3 + Fe_2O_3$ (e.g. 85.0%) but virtually free of CaO (e.g. 0.8%) [26,139].

Table 2
Representative physiochemical characteristics of conventional pozzolans and solid wastes that were tested as pozzolans.

Class	Pozzolanic materials	Chemical composition (wt%), determined by X-ray fluorescence (XRF) analysis									Mean particle size μm	Median particle size (d_{50}) μm	Specific gravity 1	BET surface area m^2/g	Ref.
		SiO_2	CaO	Al_2O_3	Fe_2O_3	MgO	K_2O	Na_2O	SO_3	LOI					
Conventional	Silica fume	94.00	0.40	0.10	0.10	0.40	0.90	0.10	1.50	2.70	0.10	–	2.16	–	[90]
Conventional	Metakaolin	52.10	0.07	41.00	4.32	0.19	0.63	0.26	0.00	0.60	–	–	2.50	–	[101]
Coal ash	Coal fly ash	53.50	3.38	20.40	8.66	0.00	0.00	0.00	0.00	0.86	13.90	–	2.25	1.20	[97]
Coal ash	Coal bottom ash	56.00	0.80	26.70	5.80	0.60	2.60	0.20	0.10	4.60	35.00	–	2.00	–	[26]
Biomass ash	Rice husk ash	84.75	2.78	0.16	0.00	2.32	2.57	0.37	0.60	3.72	–	10.00	2.16	–	[119]
Biomass ash	Palm oil fuel ash	65.30	6.40	2.60	2.00	3.10	5.70	0.30	0.50	10.10	–	10.10	2.33	–	[117]
Biomass ash	Sugar cane bagasse ash	55.00	11.00	5.10	4.10	0.90	1.20	0.20	2.20	19.60	–	5.60	2.27	–	[129]
Biomass ash	Wood ash	41.00	11.40	9.30	2.60	2.30	3.90	0.90	0.00	0.00	–	–	–	40.29	[108]
Biomass ash	Corn cob ash	66.38	11.57	7.48	4.44	2.06	4.92	0.41	1.07	0.00	–	–	–	–	[3]
Biomass ash	Switchgrass ash	67.18	12.28	0.68	0.31	2.05	1.24	0.11	0.00	14.77	65.00	–	1.79	41.25	[147]
Biomass ash	Wheat straw ash	83.80	12.54	4.55	1.05	2.39	0.00	0.00	1.49	7.22	–	–	2.41	–	[14]
Biomass ash	Olive residue ash	11.84	54.82	2.60	1.38	4.36	9.26	0.16	0.00	11.73	–	–	–	–	[33]
Biomass ash	Sawdust ash	67.20	9.98	4.09	2.26	5.80	0.11	0.08	0.45	0.00	–	–	2.29	–	[38]
Other ash	Sewage sludge ash	50.60	1.93	12.80	7.21	1.48	1.70	0.32	2.38	21.58	–	–	2.61	1.09	[94]
Other ash	Fluid bed combustion ash	35.40	23.50	12.90	3.30	1.60	1.60	0.60	10.60	8.30	–	–	–	–	[59]
Other ash	Activated alum sludge ash	47.00	0.41	41.94	4.86	0.40	0.99	0.09	0.10	2.64	–	–	2.53	–	[92]
Other ash	Cattle manure ash	52.00	15.40	7.79	3.20	2.94	4.91	0.66	1.54	2.50	–	–	0.81	0.56	[157]
Blast furnace slag	Ground granulated blast furnace slag	35.11	37.56	17.63	0.35	5.52	0.00	0.32	0.00	0.75	–	–	–	–	[74]
Other solid wastes	Fluid catalytic cracking catalyst residue	48.20	0.01	46.00	0.95	0.01	0.01	0.50	0.04	1.50	–	–	2.42	–	[101]
Other solid wastes	Zeolite	67.79	1.68	13.66	1.44	1.20	1.42	2.04	0.50	0.00	–	–	2.20	–	[12]
Other solid wastes	Glass powder	72.80	4.90	1.40	0.00	3.40	0.30	16.30	0.00	0.00	150.00	–	2.40	–	[120]
Other solid wastes	River sand	91.20	0.70	1.80	0.20	0.10	2.30	0.10	0.00	1.80	–	2.20	2.61	–	[128]
Other solid wastes	Milos earth	58.23	7.40	14.22	4.31	1.43	2.24	1.30	1.16	0.00	–	–	–	–	[96]
Other solid wastes	Diatomaceous earth	22.33	45.89	0.96	1.00	1.54	0.10	0.32	1.24	0.00	–	–	–	–	[96]
Other solid wastes	Silica breccia	82.10	0.83	8.78	0.82	0.04	3.10	2.33	0.00	0.70	75.00	–	2.70	–	[58]
Other solid wastes	Tincal ore waste	17.11	16.94	2.61	0.41	15.40	1.05	0.21	0.00	28.90	–	–	2.41	–	[75]
Other solid wastes	Ceramic Waste	67.03	0.11	19.95	6.29	1.37	3.54	0.21	0.00	0.47	–	–	–	3.00	[115]
Other solid wastes	Slate waste	62.74	1.13	18.55	6.80	2.30	4.26	1.18	0.21	0.00	–	63.00	–	–	[44]
Other solid wastes	Refinery waste catalyst	39.20	0.10	59.40	0.00	0.00	0.00	0.00	0.00	1.30	–	–	2.60	–	[78]

Mortars with 25% bottom ash had nearly the same strength as cement-only mortars (97% after 90 d curing) [26]. A 6 h grinding period to reduce the coarse particle size of bottom ash considerably enhanced its PA, which made the blended mortar stronger by 27% than when mixed with untreated bottom ash.

3.2.2. Biomass ash

The ash from biomass combustion has been tested as a pozzolan, but the PA of biomass ash is more variable than that of coal ash pozzolans due to greater variability in the chemical composition of the starting material. This is due to the fact that biomass is the biological organic matter from plants or plant-based lignocellulosic materials and is grown in many different environments. Direct combustion of biomass in boilers generates steam or heat, a carbon-neutral energy source that has the potential to partially replace fossil fuel and achieve CO_2 reduction [95]. Burning 1 kg of biomass generates 0.05–0.2 kg of ash, a solid waste that is a potential pollutant due to its fine particle size and high mineral content [150]. Recycling biomass ash as a pozzolan might be an option, but the feasibility of this approach requires more careful study due to the inconsistent chemical composition of biomass ash, even when the starting material is from the same plant species. For example, switchgrass is a biomass fuel that can be harvested several times during the year, depending on the producer's objectives. The $SiO_2 + Al_2O_3 + Fe_2O_3$ content of combusted switchgrass ash varied from 44.2% to 67.9% when generated from switchgrass biomass that was harvested at different times during the growing season, between July and November [91]. This illustrates the need to fully characterize each biomass ash before it is considered for use as a pozzolan.

Rice husk ash is frequently presented as a qualified pozzolan with suitable physicochemical properties for cement products. After rice husk was combusted at 600 °C, the ash contained 91.7% SiO_2 with a specific surface area of 77.4 m^2/g. Mixing 10% of this ash with cement improved the strength of mortar by 16.8% compared to a plain mortar [151]. In addition to its pozzolanic function, the fine particle size of rice husk ash also acted as a filler, which could significantly lessen the permeability of concrete. When mixing 10% rice husk ash (88.1% $SiO_2 + Al_2O_3 + Fe_2O_3$) with cement, the air permeability of concrete decreased from 1.08×10^{-16} m^2 to 0.08×10^{-16} m^2 after 28 d curing [111]. Furthermore, an ultrafine fine rice husk ash could be used for high strength concrete

preparation. By mixing 10% ash (88.0% amorphous SiO_2, 3.6 μm mean particle size) in cement and adjusting the W/B to 0.18, the compressive strength of concrete reached 180 MPa and 210 MPa after 28 d and 91 d curing, respectively [136]. This indicates that rice husk ash is a competitive substitute for the ultra-fine amorphous silica fume (conventional pozzolan), which has limited availability worldwide and is more costly than rice husk ash [136].

Palm oil fuel ash also showed a competitive pozzolanic function owing to its high $SiO_2 + Al_2O_3 + Fe_2O_3$ content (45.8–79.1%) [20,29,118]. Ultrafine ash from combusted palm oil fuel was an efficient pozzolanic additive that produced high strength concrete. Replacing 40% or 50% of Portland cement by this ash (75.14% $SiO_2 + Al_2O_3 + Fe_2O_3$, 2.06 μm median particle size) produced a concrete sample with compressive strength higher than 104 MPA or 158 MPa at 28 d [4,71]. The filler effect of the ultrafine particles contained in palm oil fuel ash further decreased the porosity of concrete, thus lowering its permeability to chloride, air and water [71]. When 70% cement substitution with palm oil fuel ash (67.18% $SiO_2 + Al_2O_3 + Fe_2O_3$) was tested, this ash effectively minimized the thermal cracking risk by diminishing the hydration heat release from 57.3 °C to 41.5 °C [10].

Sugarcane processing wastes such as bagasse ash and straw ash might be a satisfactory pozzolan as well. Bagasse ash was rich in $SiO_2 + Al_2O_3 + Fe_2O_3$ (e.g. 71.1–73.9%), which enhanced the strength of concrete by 13% when a mixture of 20% ash and cement was tested after 28 d [30,129]. Mixing 10–30% ash could further lessen the thermal cracking risk by lowering the hydration heat release by 13–33%. Montakarntiwong et al. [85] also reported a successful outcome from mixing 20–30% bagasse ash (89.2% $SiO_2 + Al_2O_3 + Fe_2O_3$) with cement without any reduction in concrete strength. Similar to other fine pozzolans, bagasse ash also had a dual role in concrete formation by contributing to the chemical pozzolanic function and the physical filler effect [31]. Research on sugarcane straw ash concentrated mainly on its pozzolanic kinetic properties. Villar-Cociña et al. [142] developed a simple conductivity test for kinetic analysis that could distinguish whether the pozzolanic reaction was controlled by physical diffusion or by chemical equilibrium, and this method was validated by Frías et al. [45]. The results revealed that the sugarcane straw ash from 800 °C combustion had a higher pozzolanic reaction rate ($(8.12 \pm 0.67) \times 10^{-2}\ h^{-1}$) than that from 1000 °C combustion ($(6.34 \pm 0.42) \times 10^{-2}\ h^{-1}$), which implies that chemical equilibrium was the principal mechanism responsible for the PA of sugarcane straw ash [46].

Aside from the biomass ash described above, assorted biomass ashes were studied as pozzolans in a few papers, such as corn cob ash [2], olive residue ash [33], switchgrass ash [147], wheat straw ash [14], bark ash [19], bamboo ash [141] and sawdust ash [38]. Despite their different biomass sources and combustion regimes, they all possess a similar physiochemical trait, namely an amorphous SiO_2-rich crystal structure. We conclude that ash from biomass combustion with high content of amorphous SiO_2 has potential as an eligible pozzolan, comparable to coal fly ash.

3.3. Other solid wastes

Blast furnace slag is a non-metallic byproduct from iron production in blast furnace that is frequently used as a pozzolan. Blast furnace slag contains >80% amorphous crystal when the molten slag is rapidly chilled by water immersion, with 28–38% SiO_2, 30–50% CaO, 8–24% Al_2O_3 and 1–18% MgO, which indicates that it possesses both pozzolanic function and cementitious properties. Mixing 10–20% slag with cement achieved mortar strength comparable to plain mortar [134], and even boosted its chloride corrosion durability by 53.4% at 90 d [25]. The high CaO content of slag increased the alkalinity of the hydration solution, thus accelerating the dissolution of SiO_2 and boosting the pozzolanic reaction. Blast furnace slag also improved concrete durability upon exposure to extreme temperature conditions. Blending 20–30% slag in cement eased the high temperature impairment (900 °C) of concrete by up to 60% [74]. This observation was confirmed by [68], who ran a 30 cycle freeze-thaw test on mortars with 40% slag. Variability in the pozzolanic reaction of slag-cement mixtures is observed across a range of curing conditions. For instance, seawater curing was beneficial to the early strength (7 d) of the concrete from slag-cement mixtures (from 37.6 MPa to 41.3 MPa) but harmful to the 360 d ultimate strength (from 66.0 MPa to 56.3 MPa), compared to regular water curing [25]. However, slag-cement mixtures performed well in regular curing conditions and clearly improved the concrete performance, with lower operating cost owing to less cement usage [50].

Another solid waste from industry that possess pozzolanic function is the fluid catalytic cracking catalyst residue (FC3R) from petroleum refineries, which is rich in reactive silica-alumina-based compounds [158]. Payá et al. [99] tested this material as a "new" pozzolan and found that FC3R contained 48.2% SiO_2 and 46.0% Al_2O_3 with semi-crystalline and crystalline structure. When mixing 30% FC3R in cement, it increased the strength of mortar by 31.8% at 28 d. FC3R also lessened the permeability of hydration products, thereby increasing chloride resistance of the steel rebar in mortar specimens [86]. These improvements were attributed to the auxiliary formation of C-S-H, C-A-H and C-A-S-H by the SiO_2 and Al_2O_3 in FC3R [101,102,103].

Other solid waste materials can exhibit a good pozzolanic function, such as paper/sewage/alum sludge ash [34,53,92], waste glass [120], river sand [128], tincal ore waste [75], calcium carbide residue [109], ceramic waste [83], English red brick dust [54], and light-emitting diode sludge [77]. Details about the chemical properties of these materials and their PA are summarized in Table S1. We conclude that pozzolanic-active materials from diverse sources (combustion ashes, blast furnace slags and other wastes) possess the same general physicochemical traits, namely a high $SiO_2 + Al_2O_3 + Fe_2O_3$ content with a fine particle size and amorphous SiO_2 structure.

There are many natural or artificial ashes that might be used as a pozzolan. For instance, ground volcanic ash is a good natural pozzolan due to its high $SiO_2 + Al_2O_3 + Fe_2O_3$ content of 83.9% [63,122]. Mortars with 10% volcanic ash exhibited practically the same compressive strength as plain mortars (27 MPa at 7 d, and 36 MPa at 28 d). In the meantime, its pozzolanic contribution lessened the ASR expansion of mortar bars from 0.089 mm (plain mortars) to 0.088 mm (20% ash), 0.082 mm (30% ash) or 0.075 mm (40% ash).

The ash from municipal solid waste (MSW) incineration can be used as cement substitute. Incineration is a common treatment of MSW, since it can reduce the waste volume up to 90% while recovering the latent heat from MSW. Blending MSW ash in concrete immobilized the heavy metal elements of ash, thereby avoiding pollution from metal leaching [125]. Fine MSW ash may be a good pozzolan. It reached a melting state after a 96 h grinding, due to the ultra-high reactive specific surface area of 79.7 m^2/g in the ash crystal [24]. Mixing this ash increased the cement paste strength by ≈4.5% (5% ash) or ≈18.2% (10% ash) at 28 d. This improvement in cement paste was exclusively attributed to the supplemental formation of C-S-H by pozzolanic reaction.

4. Improvement of pozzolanic activity in solid wastes

There are several effective methods to improve the PA of solid wastes, such as optimizing the combustion that produces pozzolanic ash, adding chemicals during cement hydration, elevating the curing temperature, or pretreating the pozzolans (longer

grinding time to reduce particle size, washing step to improve the purity of $SiO_2 + Al_2O_3 + Fe_2O_3$). In all cases, these methods aim to increase the $SiO_2 + Al_2O_3 + Fe_2O_3$ content and amorphous crystal proportion of pozzolans.

4.1. Combustion optimization

Combustion conditions alter the physiochemical properties of ash, thus potentially changing its PA. Factors such as the combustion temperature, retention time and cooling method determine the carbon removal degree during combustion (thus affecting the $SiO_2 + Al_2O_3 + Fe_2O_3$ purity of ash) and influence the thermal-sensitive amorphous—crystalline transformation in ash. So far, the influence of these factors on PA of ash were investigated in biomass combustion studies (Table 3), since the firing conditions for other combustion ashes are set by the energy generator or iron smelter. Feng et al. [41] found that 800 °C combustion for 4 h produced a rice husk ash containing 95.7% amorphous SiO_2, the highest value achieved in their combustion trials. This ash increased the compressive strength of mortar (with 10% ash) by 42% after 91 d. However, Xu et al. [151] proposed a 600 °C combustion for 2 h for the best PA of rice husk ash. Adding 10% of this ash in mortars (W/B = 0.4) resulted in the highest compressive strength of 59.87 MPa (28 d), compared to the ash produced from combustion at 500 °C (49.82 MPa), 700 °C (47.40 MPa) or 800 °C (46.49 MPa). This apparent contradiction indicates that combustion temperature is not the sole factor that influences PA of ash, since the type of combustion furnace and cooling method also differed in these studies. Accordingly, Nair et al. [87] explored the impact of cooling on the microstructure of rice husk ash. They suggested that

Table 3
Experimental details of pozzolan testing and final recommendations for improving the pozzolanic activity of biomass combustion ash.

Materials	Initial load g	Temperature °C	Heating rate °C/min	Retention h	Combustion equipment	Grinding min	Condition recommended for the best pozzolanic activity	Ref.
Rice husk ash	—	500, 600, 700, 800	20	2	Electric oven	120	600 °C combustion	[151]
Rice husk ash	100	700	10	0.25, 1, 4, 8, 16	20 × 28 × 2 cm stainless steel tray	20	4 h combustion	[140]
Rice husk ash	—	550, 600, 700, 800, 900, 1000	—	4	—	60	800 °C combustion + 1 mol HCl washing	[41]
Rice husk ash	—	—	—	—	Designed oven	30, 60	60 min grinding + 30 min fire + 60 min air supply + 2 d cooling	[154]
Rice husk ash	—	600, 750, 900 (combustion & gasification)	—	0.5	—	—	750 °C gasification	[148]
Rice husk ash	20,000	Max. 600 (open combustion)	—	—	—	—	—	[28]
Rice husk ash	20,000–25,000	—	—	—	Modified incinerator	0–540	45 min grinding	[137]
Rice husk ash	—	500, 700, 900	—	0.25, 6, 12, 24	—	—	500 °C combustion + 12 h + quick cooling	[87]
Rice husk ash	—	850	—	0.17–0.25	Boiler	75	—	[23]
Rice husk ash	—	750, 830	—	—	—	—	750 °C combustion + extra air supply	[90]
Rice husk ash	20,000	Max. 650	—	—	Open burning in small heap	—	—	[29]
Rice husk ash	—	650	3.3	1	Industrial furnace	—	—	[47]
Wheat straw ash	200	500, 650, 700, 800	—	1, 2, 3	Programmable electric muffle furnace	60	650 °C/1 h combustion + 80 °C/24 h 0.1 mol/L HCl washing	[7]
Wheat straw ash	—	670	—	5	Electric furnace	—	Quick cooling after combustion	[14]
Wheat straw ash	—	570, 670	—	5	Steel trays	—	670 °C combustion	[57]
Bagasse-rice husk-wood ash	—	700–900	—	—	—	—	Grinding until <2% particle retained on sieve No. 325	[62]
Rice husk-bark ash & palm oil fuel ash	—	800–900	—	—	Fluidized bed combustion	—	Grinding until <3% particle retained on sieve No. 325	[117]
Palm oil fuel ash	—	500 ± 50	—	1.5	Gas furnace	—	Grinding to the median particle size of 2.06 μm	[71]
Palm oil fuel ash	—	800–1000	—	—	Steam power plant	—	Grinding until <3% particle retained on sieve No. 325	[131]
Paper sludge	—	600, 650, 700, 750, 800	—	2, 5	Electric laboratory furnace	—	700 °C/2 h combustion	[48]
Paper sludge	—	700, 720–740	—	2	Lab furnace, fluidized bed combustion system	—	700 °C/2 h combustion in lab furnace	[43]
Paper sludge	—	700	—	2	Electric laboratory furnace	—	—	[53]
Banana leaves ash	—	900	—	24	—	30	—	[73]
Slate waste	—	1000	—	2	Electric furnace	—	—	[44]
Activated alum sludge ash	—	800	5	2	Electric laboratory furnace	—	Pretreatment of 105 °C/24 h thermal activation	[92]
Bioethanol byproduct (corn stover)	200	500, 650	—	1, 2	—	—	500 °C/2 h combustion + 80 °C/4 h 0.1 mol/L HCl washing	[8]
Switchgrass ash	492–1323	≈411	—	0.083	Lab-designed furnace	0.5	Adding 5% Na_2SO_4 or 5% $CaCl_2{\cdot}2H_2O$	[147]
Sugar cane straw ash	—	800, 1000	—	0.3	Electric furnace	—	800 °C combustion	[46]
Corn cob ash	—	650 (open air combustion)	—	8	Blacksmith furnace	—	—	[1]
Bamboo leaf ash	—	600	—	2	Electric furnace	—	Grinding to <90 μm of particle	[141]

combustion at 500 °C for 12 h, with a quick cooling by immediately removing ash from oven, was important to preserve the amorphous SiO_2 content. Quick cooling resulted in greater amorphous ash structure, improving the PA of ash by 1.9%, compared to slow cooling (ash was allowed to cool to room temperature within the oven). Furthermore, retention time within the combustion furnace (30–60 min), air supply duration (60–105 min) and cooling time (1–2 d) interacted to affect the PA of rice husk ash [154]. Rice husk ash contained the highest SiO_2 content of 86.5% and lowest C content of 3.21% when the retention, air supply and cooling times were 30 min, 60 min and 2 d, respectively.

Combustion conditions that influenced the PA of rice husk ash are relevant to other biomass sources. For example, wheat straw ash produced from 670 °C combustion made the cement pastes stronger by 11.5% than that generated at 570 °C [14]. As well, combustion at 700 °C for 2 h produced paper sludge ash with the best PA [48], resulting in CH depletion of 14.2 mmol/L with ash under the 700 °C/2 h conditions, compared to 700 °C/5 h ash (≈12.4 mmol/L), 750 °C/2 h ash (≈12.6 mmol/L), or 750 °C/5 h ash (≈11.8 mmol/L). Clearly, there is an interactive effect of combustion temperature and time on PA, which led other researchers to consider these two parameters in optimizing combustion conditions for high PA with corn stover bioethanol residue ash [8] and sugar cane straw ash [46], among others. However, there is still no consensus on the recommended combustion parameters to maximize PA in biomass combustion ash, even when the same biomass is used. The inconsistency in the scientific literature is ascribed to the fact that researchers do not follow a standard experimental protocol in biomass combustion tests, thus furnace type, ignition manner, airflow ventilation and other uncontrolled factors influence the PA of the biomass combustion ash.

4.2. Chemical addition during hydration

4.2.1. Hydration accelerator

Since the pozzolanic reaction is strongly associated with cement hydration, some accelerators used for hydration may change the PA. Common hydration accelerators are Na_2SO_4, K_2SO_4, Na_2SO_3, $CaSO_4$, $CaCl_2$ (or $CaCl_2{\cdot}2H_2O$) and NaOH. Shi and Day [122] blended 4% Na_2SO_4 or 4% $CaCl_2{\cdot}2H_2O$ with cement to increase the PA of volcanic ash by 83.3% (Na_2SO_4) and 87.5% ($CaCl_2{\cdot}2H_2O$) at 270 d. Na_2SO_4 improved the PA at early curing age (X d) by accelerating the CH consumption, but did not contribute any enhancement thereafter. Conversely, $CaCl_2{\cdot}2H_2O$ enhanced the PA throughout 270 d curing period. Shi and Day [124] studied the functions of these accelerators in CH—volcanic ash—water mixtures and found that 4% Na_2SO_4 reacted with CH in the following manner (Eq. (8)):

$$Na_2SO_4 + Ca(OH)_2 \rightarrow CaSO_4 \cdot 2H_2O + NaOH \quad (8)$$

Consequently, the formation of NaOH promoted the alkali dissolution of SiO_2 in the pozzolan, thereby accelerating the rate of pozzolanic reaction [156]. On the other hand, cement mortar containing $CaCl_2{\cdot}2H_2O$ (or $CaCl_2$) rapidly formed a new crystal $(CaO)_3{\cdot}Al_2O_3{\cdot}CaCl_2{\cdot}10H_2O$—$(CaO)_3{\cdot}Al_2O_3{\cdot}Ca(OH)_2{\cdot}12H_2O$ around the C-S-H gel. This crystal was stronger and denser than C-S-H, which developed the strength and durability of concrete. However, the high concentration of dissolved $CaCl_2$ reduced the pH in cement-pozzolan-accelerator mixtures, thus retarding the SiO_2 alkali dissolution. Consequently, the $CaCl_2{\cdot}2H_2O$ accelerator did not contribute to the early strength of cement paste but improved the late strength of cement (Shi and Day [123]). K_2SO_4 had a similar function as Na_2SO_4 due to the SO_4^{2-} ion [104], such that both 4% Na_2SO_4 and 4% K_2SO_4 increased the hydration degree from 14.2% to between 21.0 and 22.3%. Enhanced (hydration improved the PA by ≈55.5% (Na_2SO_4) or ≈47.8% (K_2SO_4) after 90 d of curing. The proportions of chemical accelerators that benefit the development of cement strength included 3% Na_2SO_4 (Zhang et al. [156]), 5% Na_2SO_4 (Wang et al. [147]) and 1% K_2SO_4 (Gastaldini et al. [49]). Moreover, several other chemicals also proved feasible, including 6–14% $CaSO_4$ [105], 1% Na_2SiO_3 [49], or NaOH-based synthesized compounds [27,153]. Adding these chemicals would have an effect akin to Na_2SO_4, which created a stronger alkali environment that might stimulate the formation of more crystalized CH or intensify the SiO_2 dissolution from pozzolans.

4.2.2. Other chemicals

In addition to the conventional hydration accelerators mentioned above, several emerging materials can improve the PA of pozzolans. For instance, 5–15% polypropylene fiber enhanced the PA of metakaolin and zeolite, which made blended concrete (5–10% pozzolan) more resistant to $MgSO_4$ attack [12]. Adding ⩽10% of waste aluminosilicate catalyst improved the PA of fly ash due to a faster hydration rate in the early phases of curing [149]. Amendment with 3% polyvinyl alcohol lessened the porosity of the cement paste with rice husk ash due to the formation of supplementary amorphous compounds [127]. Addition of 2.25–5% colloidal nanosilica containing ~100% amorphous SiO_2 reinforced the early strength of cement—fly ash mortars [65]. Increasing the mixing ratio of this nanosilica was consistently beneficial to the mortar strength in early stages, but adversely affected the long-term strength after 3 months. The reason for the loss of physical strength in concrete was not determined by Hou et al. [65], and remains to be explained.

4.3. Elevation of curing temperature

As hydration is a temperature-sensitive and exothermic process, PA might be altered by different curing temperatures [121]. Most studies thus far stated that a higher curing temperature was advantageous, especially for short-term PA. For example, Narmluk and Nawa [88] found that a higher curing temperature (50 °C) improved the PA of coal fly ash in mortars by 6 times that measured at room temperature (20 °C) because it shortened the time to initiate the pozzolanic reaction from 28 d to 12 h. However, the higher curing temperature (23–65 °C) merely increased the pozzolanic reaction rate, as verified with pozzolanic kinetic analysis [123], but did not alter any composition or microstructure of concrete. Conversely, Rojas and Sánchez de Rojas [112] argued that the better PA of metakaolin at a 60 °C curing was attributed to greater amorphous content of stratlingite ($Ca_2Al_2(SiO_2)(OH)_{10}{\cdot}2.5(H_2O)$) in hydration products caused by the higher curing temperature. These disparities warrant further evaluation of the hydration products and pozzolanic reaction kinetics as a function of temperature.

The practicability of elevating the curing temperature for a better long-term PA was evaluated by several authors. Compared to curing at 20 °C, Hanehara et al. [56] reported that a 40 °C curing could increase the PA of fly ash by 33.3% after 1 year. The blended mortars (20% or 30% fly ash) had higher long-term strength with curing at 40 °C (55.0 or 55.2 MPa) than at 20 °C (53.2 or 46.5 MPa). Yet, a 40 °C curing was rather harmful to plain mortars, and weakened the strength from 51.0 MPa to 44.7 MPa. This was explained by the lower thermal expansion in the compact microstructure of blended mortars, which did not weaken at elevated curing temperatures [81]. Similar conclusions were reached by Escalante-Garcıa and Sharp [39] and Ezziane et al. [40] with curing temperatures of 10–60 °C for mortars containing volcanic ash, ground granulated blast furnace slag and natural pozzolan.

No consistent correlation between curing temperature and PA has emerged thus far, due to the complexity of reaction kinetics in the cement—pozzolan—water system. In light of this need,

Payá et al. [100] developed a model that addressed several key factors, including curing temperature (T) (20–80 °C), cement replacement percentage by fly ash (R) (10–60%), and the compressive strength of blended mortar (S) (Eq. (9)).

$$S = a + b \times R + c \times (T - d)^2 + e \times R \times T \quad (9)$$

where a, b, c, d and e were the model coefficients, listed in Table 4. Consequently, this model mathematically advised a 50–60 °C curing to obtain the strongest blended mortar. While it is possible experimentally to obtain a better PA by using a higher curing temperature, we do not recommend this strategy, especially for a large-scale application. The principal reason to discourage a higher curing temperature is that increasing the water temperature during the curing would consume more external energy, particularly in the cold-climate zones where the air temperature could easily fall below −10 °C during construction and building activities (e.g. Canada, Russia and Scandinavian countries).

4.4. Pretreatment of alternative pozzolanic materials

4.4.1. Longer grinding

Prolonging the grinding time of a pozzolan is beneficial to its PA, since finer particle size increases the reactive surface area of pozzolan and provides a filler effect in the microstructure of concrete. For example, a 60 min grinding could make ⩾90% rice husk ash pass a 45 μm sieve [154]. Cordeiro et al. [31] systematically investigated the correlation among the grinding time, median particle size, Blaine fineness, PA and Ca^{2+} consumption capacity of sugar cane bagasse ash (Fig. 1). A finer particle size (from 76.3 to 1.7 μm) consistently resulted in better PA (49–103%). The improvement of PA enhanced the strength of mortars via promoting CH consumption in the pozzolanic reaction (36–298 mg CaO/g). Longer grinding (10–120 min) increase the exterior surface area (496–979 m^2/kg) of sewage sludge ash, however, it did not affect its crystalline constituent, specific gravity and internal surface area. Finer sewage sludge ash also acted as a lubricant in the microstructure of mortar, thus improving its workability by ≈20% [94]. Conversely, Givi et al. [51] hold an opposite view towards the fineness of ash and the workability of concrete, based on their study with rice husk ash. Mixing 5–20% of fine ash (5 μm by 180 min grinding) improved the strength but reduced the workability of concrete. Their explanation was that a coarser ash particle was absorbed on the oppositely charged surface of cement particles, which restricted flocculation of these particles. Consequently, the cement particles were dispersed and could capture a larger amount of water, which reduced the water requirement to obtain a satisfactory consistency. This explanation was substantiated by Van et al. [137], who found that finer rice husk ash absorbed part of the aqueous phase from the C-S-H gel, thus decreasing the effective water content. Since the ash can retain water within its microstructure, longer grinding time that reduces the water-holding capacity of the ash pores would reduce PA, as demonstrated when comparing a ⩾120 min grinding, which reduced the pore volume of ash to 116.4 mm^3/g, with a 45 min grinding that yielded 135.1 mm^3/g [137]. This implies that the best grinding pretreatment for a pozzolan must not simply consider the direct effect of particle size on PA and as a filler in concrete, but also how the mortar workability and water adsorption are affected by the pozzolan particle size.

Table 4
Model coefficients (a, b, c, d and e) and standard deviation (δ) derived by Eq. (9) to address the correlations among curing temperature, cement replacement by fly ash (R), and the compressive strength of blended mortar, modified from the work of Payá et al. [100].

R (%)	a	b	C	d	e	δ (MPa)
0	39.55	−0.403	−0.00567	68.41	0.00169	2.3
10	40.80	−0.419	−0.00727	62.87	0.00219	2.5
40	40.98	−0.396	−0.00768	62.46	0.00302	3.0
60	42.07	−0.383	−0.00866	61.85	0.00278	2.7

4.4.2. Thermal and acid washing

Thermal and acid washing pretreatments aim to alter the chemical composition of pozzolans by heating (to remove carbon) or washing (to remove alkali metal oxides and phosphate), leading to a higher purity of $SiO_2 + Al_2O_3 + Fe_2O_3$ that makes the pozzolans more reactive. For instance, palm oil fuel ash heated at 500 ± 50 °C for 90 min in a gas furnace contained less carbon, based on Loss on Ignition (LOI) results of 2.62% in treated ash than untreated ash (21.6%) [71]. Although treating the palm oil fuel ash at 500 °C for 1 h reduced the LOI content from 9.88% to 2.20%, this pretreatment did not result in any amorphous-crystalline transformation or particle agglomeration [20,21], so the treatment simply improved the purity of the pozzolan. Acid washing of pozzolans is commonly achieved with dilute HCl or H_2SO_4 solution (1–4 mol/L). Acid

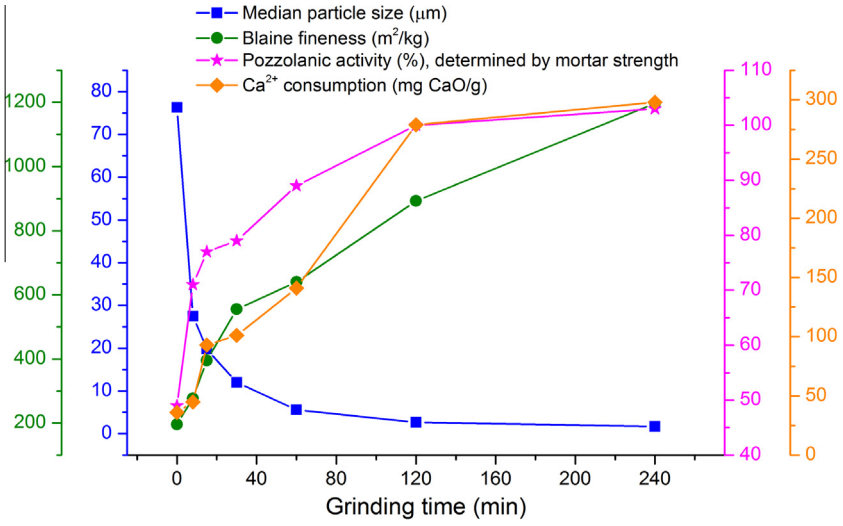

Fig. 1. Correlation among the grinding time, median particle size, Blaine fineness, pozzolanic activity, and Ca^{2+} consumption capacity of sugar cane bagasse ash, modified from the work of Cordeiro et al. [31].

washing can be implemented before or after the combustion that produces the pozzolanic ash, as both methods effectively remove soluble alkali metalsK, giving similar removal rates of Na_2O and K_2O [36,41,113].

Despite the effectiveness of these pretreatments in controlled laboratory experiments, we do not recommend either to improve the PA of combustion ash at a commercial scale. Pretreatments imply extra energy requirements to heat or dry the pozzolans after washing. Besides, the liquid waste generated from acid washing is an environmental pollutant due to its high concentration of chloride and sulfate. These drawbacks contradict the original rationale for reusing solid wastes as pozzolans, which is to minimize the waste volume and to diminish the GHG emissions from energy and cement consumption without increasing economic costs.

5. Predictive models of pozzolanic activity

Experimental studies show that there are many solid waste materials that could be used as pozzolans. These data may be used to develop screening tools as rapid indicators of pozzolanic potential in solid wastes prior to undertaking strength tests and other experimental testing. Hence, the objectives of the next sections are to 1) create a comprehensive database of the existing experimental data, and 2) develop predictive models that forecast the PA of an untested material.

5.1. Data selection and model objective

Experimental data were gathered describing the pozzolanic effect of non-conventional pozzolans – namely combustion ash, blast furnace slag and other solid wastes – on the compressive strength of concrete and mortar (Table S2). This dataset was compiled from 707 groups of test results derived from 81 papers published in peer-reviewed journals from 1998 to 2014. Testing methods in these papers conformed to internationally recognized standards, such as ASTM C 311-07, ASTM C109, NF EN 196-1 and EN 1015-11:1999. The dataset represented a diverse group of pozzolans from solid wastes that were described in Section 2, including fossil and biomass fuel ash, blast furnace slag, catalyst waste, river sand, and many others. The major assumption was that the data were scientifically accurate and unbiased, thus assuring the validity and representativeness of predictive results across a wide range of candidate pozzolanic materials.

All pozzolans possess a high $SiO_2 + Al_2O_3 + Fe_2O_3$ content with amorphous structure and fine particle size, which was described by providing their chemical composition and physical property (specific gravity) in our model. The factors that may affect the PA (as independent input variables) included the chemical composition and specific gravity of pozzolans, water-binder ratio (W/B), replacement ratio of cement by pozzolanic material and superplasticizer mixing ratio (a common additive to improve the flow characteristics of cement pastes) (Table 5). Please note that few papers in the scientific literature provide details on the amorphous content of pozzolans. No standard method exists to quantify the amorphous content of such materials, and this parameter is estimated by empirical methods in virtually all literature on the topic. Including this parameter in the ANN model would require us to limit the dataset to studies with amorphous content estimates, which would significantly reduce the number of data points in the analysis. To consider the broadest set of pozzolans and minimize uncertainty associated with this ill-defined parameter, we did not include the amorphous content of pozzolans and instead relied upon the input parameters shown in Fig. 2 for predicting PA with our ANN model. Since compressive strength was the most common response variable used to evaluate the pozzolanic effect in the literature, we included data on the compressive strength at 3, 7, 28 and 90 d to reflect the changes in pozzolanic function during early to later curing stages. To eliminate the interference from different experimental conditions in each paper (e.g. curing temperature, moisture, casting dimension, etc.), the PA was normalized by comparing the compressive strength of mortar from cement: pozzolan blends to that of 100% Portland cement, from the same study (Eq. (10)).

Table 5
Summary of input variables describing the physicochemical characteristics of pozzolans and their use in blended cement, as well as the compressive strength of cement mortar after 3, 7, 28 and 90 d curing, used in the development of an artificial neural network model to predict pozzolanic activity. The descriptive statistics from n = 707 experimental studies included the range (maximum, Max. and minimum, Min.) and the standard deviation (S.D.).

	Unit	Max.	Min.	Mean	Median	S.D.
Input variables						
SiO_2	wt%	99.80	11.84	66.43	65.60	20.98
CaO	wt%	54.82	0.01	7.03	3.00	9.47
Al_2O_3	wt%	59.40	0.01	10.33	4.40	12.76
Fe_2O_3	wt%	40.19	0.03	3.37	2.13	4.19
MgO	wt%	23.50	0.01	2.10	1.30	2.51
K_2O	wt%	25.41	0.01	2.60	2.00	2.56
Na_2O	wt%	16.30	0.01	0.77	0.37	1.72
SO_3	wt%	12.20	0.02	1.26	0.68	1.69
Loss on Ignition	wt%	28.90	0.03	5.27	3.72	5.23
Specific gravity	1	3.25	0.13	2.32	2.31	0.29
Water-binder ratio	1	0.80	0.19	0.47	0.50	0.11
Replacement ratio	%	70.00	1.00	22.17	20.00	12.88
Superplasticizer mix	%	8.50	0.10	1.37	1.03	1.28
Test results						
Compressive strength 3 d	MPa	131.38	4.32	32.09	25.67	22.11
Compressive strength 7 d	MPa	127.15	1.00	39.60	34.10	22.53
Compressive strength 28 d	MPa	131.08	3.20	50.18	45.45	22.69
Compressive strength 90 d	MPa	136.90	6.10	59.78	54.40	24.52

$$PA(\%) = \frac{\text{Compressive strength of blended sample}}{\text{Compressive strength of plain sample}} \times 100 \qquad (10)$$

Since compressive strength is typically evaluated several times during curing, the PA (%) was calculated at 3, 7, 28 and 90 d of curing time, when the data were available (n = 146). Based on this dataset, the following models aimed to 1) develop an ANN for PA prediction at different curing ages, using concrete compressive strength as an indicator of PA and the physiochemical and mixing parameters of a pozzolan as predictive variables, and 2) investigate the correlation between PA, an indicator of concrete compressive strength, and curing age with a time-series model.

5.2. Artificial neural network (ANN) description

A feed forward back-propagation ANN was constructed for PA prediction (Fig. 2). Briefly, the signals move in one direction in this model from the input layer, through the hidden layer and to the outputs. There is neither cycle nor loop among the entire processing elements (PEs). Further information on the rationale and algorithm for this method of ANN is found in Jain et al. [70], Zhang et al. [155], Basheer and Hajmeer [11], and Duan et al. [37]. The PEs in this model were arranged in layers. The PEs in each layer were wholly linked to all of the PEs in successive layers, but there was no PEs connection in the same layer. The input to a PE was obtained by multiplying the output of connected PEs by the synaptic strength of connections. Thus, the weighted sums of input $(net)_j$ for the jth PE were calculated with a linear sum function (Eq. (11)) [116].

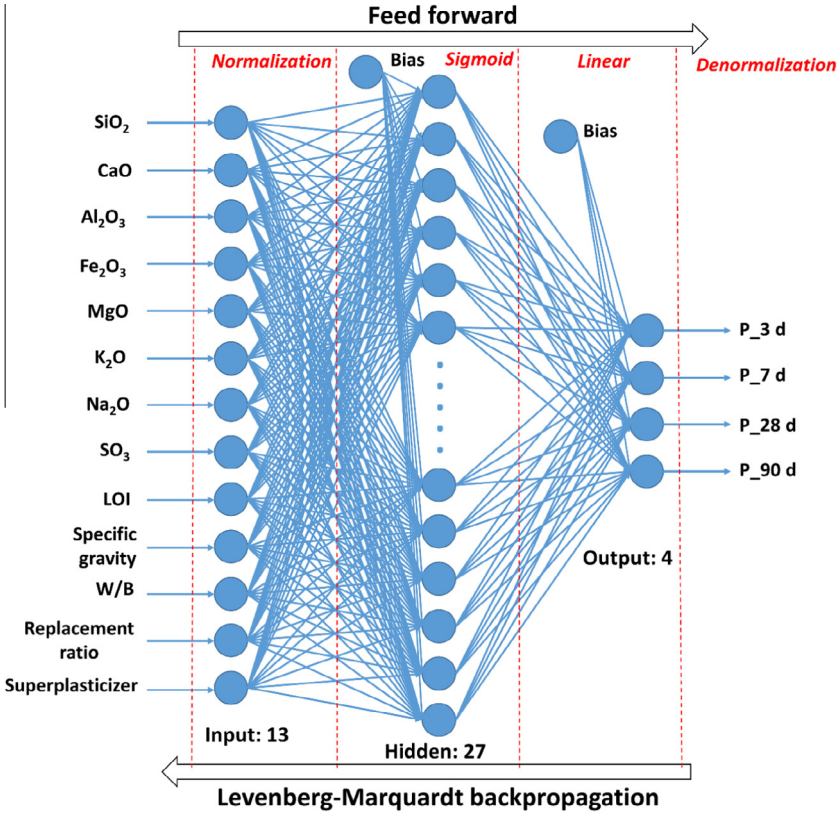

Fig. 2. Schematic structure of feed forward artificial neural network (ANN), with back-propagation algorithm, designed to predict the pozzolanic activity of blended cement containing up to 50% pozzolan from non-conventional sources (described in Table 2). P symbolized the pozzolanic activity at 3, 7, 28 and 90 d curing age.

$$(net)_j = \sum_{i=1}^{n} w_{ij} \times o_i + b_i \tag{11}$$

where the jth PE received the signals from the preceding layer containing n PEs, with the weight of w_{ij}. The output, o_i was derived from the ith PE in the preceding layer and b_j symbolized the bias that simulated a threshold value. Accordingly, the output o_j was transformed from the sum function $(net)_j$ via an activation sigmoid function (f(·)) in the PEs of hidden layer (Eq. (12)). A constant α was also used to control the slope of the semi-linear region.

$$o_j = f((net)_j) = \frac{1}{1 + e^{-\alpha \times (net)_j}} \tag{12}$$

The learning of this ANN was supervised by a back-propagation method with Levenberg-Marquardt algorithm [5]. Based on a gradient descent principle, when the errors for a particular training pattern were passed backwards from output to input layer, these errors were minimized by adjusting the weights and biases for each PE (Eq. (13)).

$$w_{ij}(m+1) = w_{ij}(m) + \eta(\delta_j \times o_j) + \beta \times w_{ij}(t) \tag{13}$$

where δ_j was the error signal of the jth PE, and m was the number of iterations. η and β corresponded to the learning and momentum rates. η was obtained by the partial derivative of the error function in Eq. (14), as shown in Eq. (15) and (16).

$$E_r = \frac{1}{2} \times \sum_j (t_j - o_j)^2 \tag{14}$$

$$\delta_j = o_j \times (t_j - o_j) \times (1 - o_j) \tag{15}$$

$$\delta_j = o_j \times (1 - o_j) \times \sum_k (\delta_k \times w_{kj}) \tag{16}$$

where t_j was the target output of the jth PE and k represented the kth layer that was the upper layer of the jth layer within the whole network model. The training process was successfully completed when the iterative process converged. Two indices were used to assess model performance, namely the root-mean-squared error (RMS) (Eq. (17)) and the root of absolute variance fraction (R) (Eq. (18)).

$$RMS = \sqrt[2]{\frac{1}{p} \times \sum_i |t_i - o_i|^2} \tag{17}$$

$$R = \sqrt[2]{1 - \frac{\sum_i |t_i - o_i|^2}{\sum_i |o_i|^2}} \tag{18}$$

where t and o were the target and predicting values of the ith pattern (with the pattern number p). A value of RMS or R that approached 0 or 1 suggested a good predictive performance.

This feed forward back-propagation ANN had an input layer, a hidden layer and an output layer (Fig. 2). The input layer contained 13 nodes that described the pozzolan and cement strength factors listed in Table 5. The output layer had 4 nodes to describe the PA prediction at 3, 7, 28 and 90 d curing. Since there is no standard method to designate the node number in hidden layer, we had to run a few trials (1–40 nodes in this study) to select this parameter [98]. As a result, a 27 node hidden layer was optimal and gave the lowest root mean square error (Fig. 3). As the sigmoid function in hidden layer ranged from −1 to 1, input layer was normalized after it was loaded with initial data, and output layer was denormalized following the sigmoid transformation [60]. Based on this topology, 70% and 15% data (selected randomly) were used for ANN training

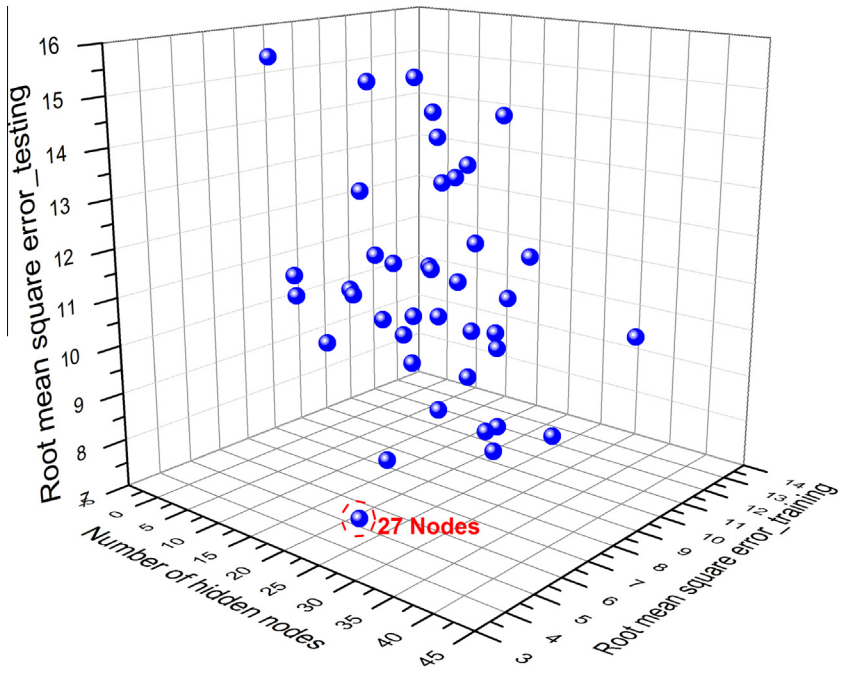

Fig. 3. Determination of the node number in the hidden layer based on the lowest root mean square error from the training and test steps. Since there was no clear method to designate the node number in the hidden layer, a few trials (1–40 nodes in this study) had to be run to select this parameter.

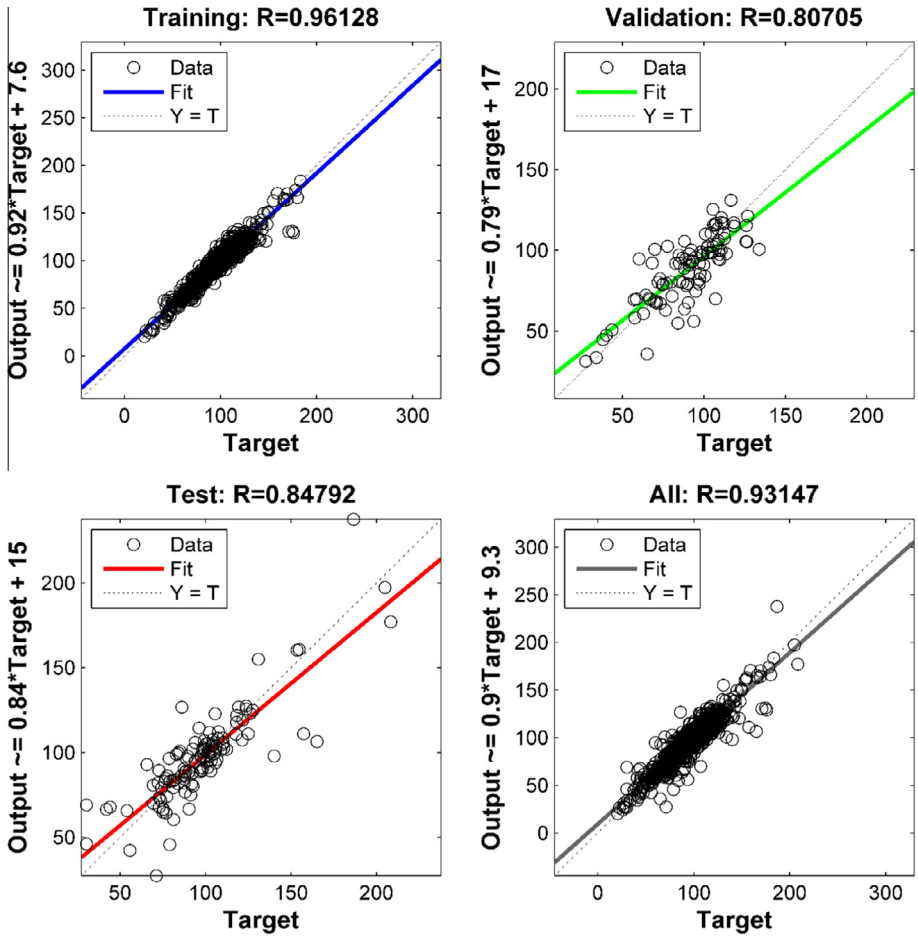

Fig. 4. Predictive results of pozzolanic activity in blended cement by artificial neural network model. "Target" corresponded to the experimental results, and "output" represented the predictive results obtained from the model. As explained in the Section 5.2 above, the PA in this equation corresponds to the normalized pozzolanic activity with the unit of %.

and validation, and this left 15% data for ANN testing. Momentum and training rates were 0.9 and 0.3, and training was terminated after 1000 cycles iteration [37]. Training was replicated 20 times, and the optimal results were those with the highest R value [35]. Additionally, to compare the ANN predictive capacity to conventional regression analyses, we performed a multivariable regression model (MVR) on the same dataset with the same normalization and denormalization steps (Eq. (19)).

$$PA(\%) = \sum_{i=1}^{13} a_i \times x_i^{b_i} + e \quad (19)$$

where x_i corresponded to the 13 input variables, a_i and b_i were the regression parameters, and e symbolized an error compensation. As explained in the above paragraphs, the PA in this equation corresponds to the normalized pozzolanic activity with the unit of %. When b_i equaled to 1, this function represents a perfect linear regression (R = 1).

5.3. Artificial neural network (ANN) performance

The ANN model was able to predict the PA of 22 types of solid waste materials with diverse physicochemical properties that underwent combustion, other heating and pretreatment before they were blended as pozzolans with cement (Fig. 4). The R^2 of 0.9613 from training step confirmed that this model was successful in learning the correlation between the input and output variables. An R value of 0.8479 from the test step was further evidence of the accuracy of predictive results. Moreover, the predictive capacity of the ANN proved superior to multivariate regression models, which were constrained by the fact that they must predict outcomes separately for each time point. This is supported by the substantially smaller root mean square value of 10.76 for the ANN compared to the regression models (38.25–42.66 at 3–90 d curing, Table 6). This implies that the complex cement—pozzolan—water system could not be described accurately with traditional regression model approach, since it cannot reflect the multiple interactions that occur among input parameters with time. We conclude that the ANN constructed in this study was a robust tool with capacity to appraise and predict the eligibility of a pozzolan for blended cement, based on its expected effect on compressive strength.

We consider our ANN to be a robust and comprehensive indicator of the PA of diverse pozzolans, but note that it is less accurate than similar models reported in the literature. Statistically, the R of 0.8479 from this ANN test indicates adequate predictive ability, but is not as close to ideal prediction as the R obtained by other ANN of pozzolans reported by Duan et al. [37] (R = 0.9977), Dantas et al. [35] (R = 0.9854), Sarıdemir [116] (R = 0.9992), and Prasad et al. [107] (R = 0.9165). This is due to the fact that our ANN relied on much broader dataset, encompassing 708 pozzolanic tests with diverse physicochemical attributes that were evaluated with multiple test methods (Table S2). Differences in the testing protocols between studies makes each experimental datapoint unique and introduces experimental error, even when similar materials or test conditions are considered, thus resulting in more variability in the dataset (Table 5). In contrast, other ANN attempting to predict PA relied on data collected under similar experimental conditions (i.e., with the same testing protocol) and even with the same pozzolan, so it is not surprising that the R values are higher for those ANN than our model. Although we attempted to normalize the data within each study by comparing the PA of blended cement with 100% cement, another option would be to normalize the PA among testing protocols. At present, we do not have sufficient information to calibrate the compressive strength of cement mortars from different test methods. In conclusion, our meta-data approach to data collection and dataset preparation yielded a robust ANN model that can be applied broadly to predict the PA of many candidate materials being considered as pozzolans,

Table 6
Comparison of the predictive error indices from multivariate regression models and an artificial neural network describing pozzolanic activity, an indicator of concrete compressive strength, after 3, 7, 28 and 90 d curing.

	Multivariate regression model				Artificial neural network
	3 d	7 d	28 d	90 d	
Root mean square error	39.19	42.66	38.35	38.25	10.76
R	0.4778	0.4517	0.5154	0.5679	0.8479

5.4. Time-series analysis of pozzolanic activity

As the compressive strengths of concrete or mortar vary considerably with different curing age, and these strengths are a reflection of the PA, the change of PA with curing age might be defined by a time-series model. The time-series equation developed by Shi and Day [122] to analyze the strength-age relationship suggests the validity of this approach, but how PA would contribute to this relationship was not discussed in their work. Assuming there is a positive linear correlation between PA and compressive strength, a time-series PA model was developed in Eq. (20),

$$P(t) = P_U \times \frac{K_T \times (t - t_0)}{1 + K_T \times (t - t_0)} \quad (20)$$

where P(t) was the PA (%) at a certain curing age t, and P_U represented a theoretical ultimate PA ($t = +\infty$). K_T (d^{-1}) meant a PA change rate constant, and t_0 (d) symbolized a theoretical initial hardening time. After calculating the mean values of n = 707 groups of PA—time data, a nonlinear data fitting was conducted with Eq. (20). Additionally, these PA—time data were statistically interpreted by a one-way Analysis of Variance (ANOVA) with Fisher's LSD tests ($P < 0.05$).

As expected, the PA increased significantly ($P < 0.05$) with curing age, from 97.21% (3 d) to 103.99% (90 d) (Fig. 5). There was little change in PA within the first 7 d, indicating a delay in pozzolanic reaction of about one week and thereafter strengthening the blended concrete (from 7 d to 90 d of curing). Cement hydration appears to be the source of compressive strength in mortar in the first week, and tended to be impaired in blended

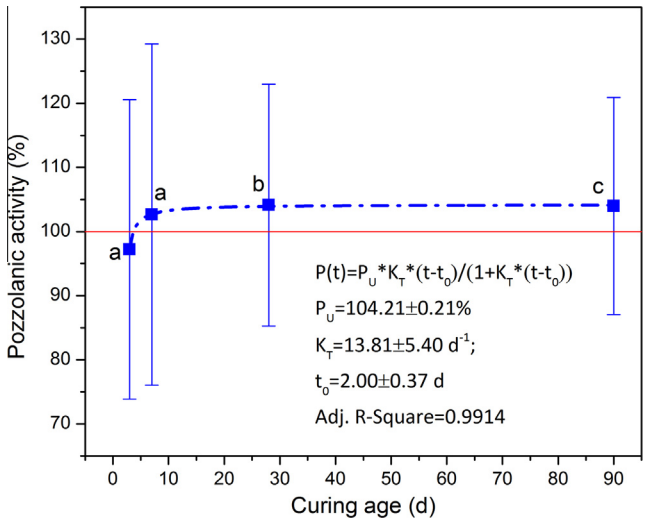

Fig. 5. Correlation between pozzolanic activity and curing age in mortar from blended cement containing 0–50% pozzolan. The value with different letters were significantly different ($P < 0.05$, Fisher's LSD test, n = 146).

cements, but this early deficiency was overcome by 7 d, when the average PA reached 100% (Fig. 5). The time-series model (Eq. (20)) was well fitted to the experimental data (Adj. $R^2 = 0.9914$), thereby confirming the suitability of this function to describe the PA—time correlation (Fig. 5). P_U was estimated at 104.21 ± 0.21% when the curing age approached $+\infty$. By solving this function versus time $(0, +\infty)$, PA would exceed 100% only if the curing is longer than 3.72 d, indicating a theoretical advantage of the pozzolanic reaction on PA after about 4 d curing. Thereafter, the PA reaction in cement-pozzolan-water system could enhance the compressive strength of the mortar after a sufficiently long curing age.

Although the mean values of PA fit well to the predictive equation of the time-series model, the standard deviation was judged to be large, owing to the wide range of physico-chemical characteristics of pozzolans and experimental conditions represented in our database (Table 5). The high variance in our time-series model indicates that it could over- or under-estimate the optimal curing times to reach critical strength when specific pozzolans are used. However, it does provide insight into the general performance that can be expected from pozzolans derived from solid waste materials. Thus, our model could be considered as a reference case or guideline for the performance of alternative pozzolans.

6. Concluding remarks

Numerous solid wastes have potential for use as pozzolans in blended cement. An acceptable pozzolan should be significantly rich in amorphous SiO_2, Al_2O_3 and Fe_2O_3, and its particle size should be fine enough to assure a highly reactive crystal surface. Blending these materials with cement saves raw materials, fuel and energy due to less Portland cement use, and achieves equivalent or superior concrete properties. ANN and time-series models accurately predict the PA of solid wastes during 3-90 d curing, thus could be used as a screening tool for waste materials being considered as potential pozzolans before undertaking strength tests.

Future studies should develop 1) a standardized and unbiased protocol for testing the PA of waste materials, thereby circumventing the disparities that arise from multiple PA assessment methods, and 2) robust correlations among the pozzolan properties, curing age and PA, which provides predictive models with more trustworthy data.

Acknowledgments

This research was funded by Natural Science and Engineering Research Council (NSERC) of Canada through grant number EGP 466286-14, and the McGill Collaborative Research Development Fund. We appreciated the industrial support from Lafarge Cement North America. We also would like to thank Dr. Chun-Chieh Yang at the United States Department of Agriculture for reviewing and providing helpful comments on the ANN methodology, results and interpretation.

Appendix A. Supplementary data

Supplementary data associated with this article can be found, in the online version, at http://dx.doi.org/10.1016/j.conbuildmat.2016.07.031.

References

[1] D. Adesanya, A. Raheem, Development of corn cob ash blended cement, Constr. Build. Mater. 23 (1) (2009) 347–352.
[2] D. Adesanya, A. Raheem, A study of the permeability and acid attack of corn cob ash blended cements, Constr. Build. Mater. 24 (3) (2010) 403–409.
[3] D. Adesanya, A. Raheem, A study of the workability and compressive strength characteristics of corn cob ash blended cement concrete, Constr. Build. Mater. 23 (1) (2009) 311–317.
[4] M. Aldahdooh, N. Muhamad Bunnori, M. Megat Johari, Development of green ultra-high performance fiber reinforced concrete containing ultrafine palm oil fuel ash, Constr. Build. Mater. 48 (2013) 379–389.
[5] Ampazis, N., Perantonis, S.J. Levenberg-Marquardt algorithm with adaptive momentum for the efficient training of feedforward networks. *Neural Networks, 2000. IJCNN 2000, Proceedings of the IEEE-INNS-ENNS International Joint Conference on* IEEE., (2000) pp. 126–131.
[6] ASTM, C618-12a: Standard Specification for Coal Fly Ash and Raw or Calcined Natural Pozzolan for Use in Concrete, 2012. West Conshohocken, PA.
[7] F.F. Ataie, K.A. Riding, Thermochemical pretreatments for agricultural residue ash production for concrete, J. Mater. Civil Eng. 25 (11) (2012) 1703–1711.
[8] F.F. Ataie, K.A. Riding, Use of bioethanol byproduct for supplementary cementitious material production, Constr. Build. Mater. 51 (2014) 89–96.
[9] U. Atici, Prediction of the strength of mineral admixture concrete using multivariable regression analysis and an artificial neural network, Expert Syst. Appl. 38 (8) (2011) 9609–9618.
[10] A. Awal, I. Shehu, Evaluation of heat of hydration of concrete containing high volume palm oil fuel ash, Fuel 105 (2013) 728–731.
[11] I. Basheer, M. Hajmeer, Artificial neural networks: fundamentals, computing, design, and application, J. Microbiol. Methods 43 (1) (2000) 3–31.
[12] K. Behfarnia, O. Farshadfar, The effects of pozzolanic binders and polypropylene fibers on durability of SCC to magnesium sulfate attack, Constr. Build. Mater. 38 (2013) 64–71.
[13] D.P. Bentz, P.E. Stutzman, E.J. Garboczi, Experimental and simulation studies of the interfacial zone in concrete, Cem. Concr. Res. 22 (5) (1992) 891–902.
[14] H. Biricik, F. Aköz, F. Türker, I. Berktay, Resistance to magnesium sulfate and sodium sulfate attack of mortars containing wheat straw ash, Cem. Concr. Res. 30 (8) (2000) 1189–1197.
[15] R. Blissett, N. Rowson, A review of the multi-component utilisation of coal fly ash, Fuel 97 (2012) 1–23.
[16] BS-EN, BS EN 196-2:2013 Method of Testing Cement, Chemical Analysis of Cement, BSI, 2013.
[17] J.W. Bullard, H.M. Jennings, R.A. Livingston, A. Nonat, G.W. Scherer, J.S. Schweitzer, K.L. Scrivener, J.J. Thomas, Mechanisms of cement hydration, Cem. Concr. Res. 41 (12) (2011) 1208–1223.
[18] F. Canpolat, K. Yılmaz, M. Köse, M. Sümer, M. Yurdusev, Use of zeolite, coal bottom ash and fly ash as replacement materials in cement production, Cem. Concr. Res. 34 (5) (2004) 731–735.
[19] W. Chalee, T. Sasakul, P. Suwanmaneechot, C. Jaturapitakkul, Utilization of rice husk–bark ash to improve the corrosion resistance of concrete under 5-year exposure in a marine environment, Cem. Concr. Compos. 37 (2013) 47–53.
[20] C. Chandara, K.A. Mohd Azizli, Z.A. Ahmad, S.F. Saiyid Hashim, E. Sakai, Heat of hydration of blended cement containing treated ground palm oil fuel ash, Constr. Build. Mater. 27 (1) (2012) 78–81.
[21] C. Chandara, E. Sakai, K.A.M. Azizli, Z.A. Ahmad, S.F.S. Hashim, The effect of unburned carbon in palm oil fuel ash on fluidity of cement pastes containing superplasticizer, Constr. Build. Mater. 24 (9) (2010) 1590–1593.
[22] S. Chandrasekhar, K. Satyanarayana, P. Pramada, P. Raghavan, T. Gupta, Review processing, properties and applications of reactive silica from rice husk—an overview, J. Mater. Sci. 38 (15) (2003) 3159–3168.
[23] B. Chatveera, P. Lertwattanaruk, Durability of conventional concretes containing black rice husk ash, J. Environ. Manage. 92 (1) (2011) 59–66.
[24] C.-G. Chen, C.-J. Sun, S.-H. Gau, C.-W. Wu, Y.-L. Chen, The effects of the mechanical–chemical stabilization process for municipal solid waste incinerator fly ash on the chemical reactions in cement paste, Waste Manage. 33 (4) (2013) 858–865.
[25] H.-J. Chen, S.-S. Huang, C.-W. Tang, M. Malek, L.-W. Ean, Effect of curing environments on strength, porosity and chloride ingress resistance of blast furnace slag cement concretes: a construction site study, Constr. Build. Mater. 35 (2012) 1063–1070.
[26] M. Cheriaf, J.C. Rocha, J. Pera, Pozzolanic properties of pulverized coal combustion bottom ash, Cem. Concr. Res. 29 (9) (1999) 1387–1391.
[27] M. Chi, R. Huang, Binding mechanism and properties of alkali-activated fly ash/slag mortars, Constr. Build. Mater. 40 (2013) 291–298.
[28] P. Chindaprasirt, P. Kanchanda, A. Sathonsaowaphak, H. Cao, Sulfate resistance of blended cements containing fly ash and rice husk ash, Constr. Build. Mater. 21 (6) (2007) 1356–1361.
[29] P. Chindaprasirt, S. Rukzon, V. Sirivivatnanon, Resistance to chloride penetration of blended Portland cement mortar containing palm oil fuel ash, rice husk ash and fly ash, Constr. Build. Mater. 22 (5) (2008) 932–938.
[30] N. Chusilp, C. Jaturapitakkul, K. Kiattikomol, Utilization of bagasse ash as a pozzolanic material in concrete, Constr. Build. Mater. 23 (11) (2009) 3352–3358.
[31] G. Cordeiro, R. Toledo Filho, L. Tavares, E. Fairbairn, Pozzolanic activity and filler effect of sugar cane bagasse ash in Portland cement and lime mortars, Cem. Concr. Compos. 30 (5) (2008) 410–418.
[32] M.W. Craven, J.W. Shavlik, Using neural networks for data mining, Future Gener. Comp. Sy. 13 (2) (1997) 211–229.
[33] J. Cuenca, J. Rodríguez, M. Martín-Morales, Z. Sánchez-Roldán, M. Zamorano, Effects of olive residue biomass fly ash as filler in self-compacting concrete, Constr. Build. Mater. 40 (2013) 702–709.

[34] M. Cyr, R. Idir, G. Escadeillas, Use of metakaolin to stabilize sewage sludge ash and municipal solid waste incineration fly ash in cement-based materials, J. Hazard. Mater. 243 (2012) 193–203.
[35] A.T.A. Dantas, M. Batista Leite, K. de Jesus Nagahama, Prediction of compressive strength of concrete containing construction and demolition waste using artificial neural networks, Constr. Build. Mater. 38 (2013) 717–722.
[36] S. Donatello, A. Freeman-Pask, M. Tyrer, C. Cheeseman, Effect of milling and acid washing on the pozzolanic activity of incinerator sewage sludge ash, Cem. Concr. Compos. 32 (1) (2010) 54–61.
[37] Z. Duan, S. Kou, C. Poon, Prediction of compressive strength of recycled aggregate concrete using artificial neural networks, Constr. Build. Mater. 40 (2013) 1200–1206.
[38] A.U. Elinwa, Y.A. Mahmood, Ash from timber waste as cement replacement material, Cem. Concr. Compos. 24 (2) (2002) 219–222.
[39] J. Escalante-Garcıa, J. Sharp, The microstructure and mechanical properties of blended cements hydrated at various temperatures, Cem. Concr. Res. 31 (5) (2001) 695–702.
[40] K. Ezziane, A. Bougara, A. Kadri, H. Khelafi, E. Kadri, Compressive strength of mortar containing natural pozzolan under various curing temperature, Cem. Concr. Compos. 29 (8) (2007) 587–593.
[41] Q. Feng, H. Yamamichi, M. Shoya, S. Sugita, Study on the pozzolanic properties of rice husk ash by hydrochloric acid pretreatment, Cem. Concr. Res. 34 (3) (2004) 521–526.
[42] A. Fraay, J. Bijen, Y. De Haan, The reaction of fly ash in concrete a critical examination, Cem. Concr. Res. 19 (2) (1989) 235–246.
[43] M. Frías, R. García, R.V. de la Villa, E. Villar, The effect of binary pozzolan mix on the mineralogical changes in the ternary activated paper sludge-fly ash-Ca $(OH)_2$ system, Constr. Build. Mater. 38 (2013) 48–53.
[44] M. Frías, R. Vigil de la Villa, R. García, I. de Soto, C. Medina, M. Sánchez de Rojas, Scientific and technical aspects of blended cement matrices containing activated slate wastes, Cem. Concr. Compos. 48 (2014) 19–25.
[45] M. Frías, E. Villar-Cocina, M.I. Sánchez de Rojas, E. Valencia-Morales, The effect that different pozzolanic activity methods has on the kinetic constants of the pozzolanic reaction in sugar cane straw-clay ash/lime systems: Application of a kinetic–diffusive model, Cem. Concr. Res. 35 (11) (2005) 2137–2142.
[46] M. Frías, E. Villar-Cociña, E. Valencia-Morales, Characterisation of sugar cane straw waste as pozzolanic material for construction: calcining temperature and kinetic parameters, Waste Manage. 27 (4) (2007) 533–538.
[47] K. Ganesan, K. Rajagopal, K. Thangavel, Rice husk ash blended cement: assessment of optimal level of replacement for strength and permeability properties of concrete, Constr. Build. Mater. 22 (8) (2008) 1675–1683.
[48] R. García, R. Vigil de la Villa, I. Vegas, M. Frías, M.I. Sánchez de Rojas, The pozzolanic properties of paper sludge waste, Constr. Build. Mater. 22 (7) (2008) 1484–1490.
[49] A. Gastaldini, G. Isaia, N. Gomes, J. Sperb, Chloride penetration and carbonation in concrete with rice husk ash and chemical activators, Cem. Concr. Compos. 29 (3) (2007) 176–180.
[50] A. Gastaldini, G. Isaia, T. Hoppe, F. Missau, A. Saciloto, Influence of the use of rice husk ash on the electrical resistivity of concrete: a technical and economic feasibility study, Constr. Build. Mater. 23 (11) (2009) 3411–3419.
[51] A.N. Givi, S.A. Rashid, F.N.A. Aziz, M.A.M. Salleh, Assessment of the effects of rice husk ash particle size on strength, water permeability and workability of binary blended concrete, Constr. Build. Mater. 24 (11) (2010) 2145–2150.
[52] A.N. Givi, S.A. Rashid, F.N.A. Aziz, M.A.M. Salleh, Contribution of rice husk ash to the properties of mortar and concrete: a review, J. Am. Sci. 6 (3) (2010) 157–165.
[53] S. Goñi, M. Frias, I. Vegas, R. García, Sodium sulphate effect on the mineralogy of ternary blended cements elaborated with activated paper sludge and fly ash, Constr. Build. Mater. 54 (2014) 313–319.
[54] E.R. Grist, K.A. Paine, A. Heath, J. Norman, H. Pinder, Compressive strength development of binary and ternary lime–pozzolan mortars, Mater. Design 52 (2013) 514–523.
[55] J. Guru Jawahar, C. Sashidhar, I. Ramana Reddy, J. Annie Peter, Micro and macrolevel properties of fly ash blended self compacting concrete, Mater. Design 46 (2013) 696–705.
[56] S. Hanehara, F. Tomosawa, M. Kobayakawa, K. Hwang, Effects of water/powder ratio, mixing ratio of fly ash, and curing temperature on pozzolanic reaction of fly ash in cement paste, Cem. Concr. Res. 31 (1) (2001) 31–39.
[57] H. Hasan, F. Aköz, I.L. Berktay, A.N. Tulgar, Study of pozzolanic properties of wheat straw ash, Cem. Concr. Res. 29 (5) (1999) 637–643.
[58] A.A. Hassan, A.A. Abouhussien, J. Mayo, The use of silica-breccia as a supplementary cementing material in mortar and concrete, Constr. Build. Mater. 51 (2014) 321–328.
[59] J. Havlica, J. Brandstetr, I. Odler, Possibilities of utilizing solid residues from pressured fluidized bed coal combustion (PSBC) for the production of blended cements, Cem. Concr. Res. 28 (2) (1998) 299–307.
[60] R. Hecht-Nielsen, Theory of the backpropagation neural network, in: Neural Networks. IJCNN., International Joint Conference, IEEE, 1989, pp. 593–605.
[61] P.V.d. Heede, M. Maes, E. Gruyaert, N.D. Belie, Full probabilistic service life prediction and life cycle assessment of concrete with fly ash and blast–furnace slag in a submerged marine environment: a parameter study, Int. J. Environ. Sustain. Dev. 11 (1) (2012) 32–49.
[62] V. Horsakulthai, S. Phiuvanna, W. Kaenbud, Investigation on the corrosion resistance of bagasse-rice husk-wood ash blended cement concrete by impressed voltage, Constr. Build. Mater. 25 (1) (2011) 54–60.
[63] K.M.A. Hossain, Volcanic ash and pumice as cement additives: pozzolanic, alkali-silica reaction and autoclave expansion characteristics, Cem. Concr. Res. 35 (6) (2005) 1141–1144.
[64] K.M.A. Hossain, M. Lachemi, Strength, durability and micro-structural aspects of high performance volcanic ash concrete, Cem. Concr. Res. 37 (5) (2007) 759–766.
[65] P.-K. Hou, S. Kawashima, K.-J. Wang, D.J. Corr, J.-S. Qian, S.P. Shah, Effects of colloidal nanosilica on rheological and mechanical properties of fly ash–cement mortar, Cem. Concr. Compos. 35 (1) (2013) 12–22.
[66] D.N. Huntzinger, T.D. Eatmon, A life-cycle assessment of Portland cement manufacturing: comparing the traditional process with alternative technologies, J. Clean. Prod. 17 (7) (2009) 668–675.
[67] G.M. Idorn, Concrete Progress: From Antiquity to Third Millenium, Thomas Telford, 1997.
[68] B. Işıkdağ, İ.B. Topçu, The effect of ground granulated blast-furnace slag on properties of Horasan mortar, Constr. Build. Mater. 40 (2013) 448–454.
[69] R. Iyer, J. Scott, Power station fly ash—a review of value-added utilization outside of the construction industry, Resourc. Conserv. Recy. 31 (3) (2001) 217–228.
[70] A.K. Jain, J. Mao, K. Mohiuddin, Artificial neural networks: a tutorial, Computer 29 (3) (1996) 31–44.
[71] M. Johari, A. Zeyad, N. Muhamad Bunnori, K. Ariffin, Engineering and transport properties of high-strength green concrete containing high volume of ultrafine palm oil fuel ash, Constr. Build. Mater. 30 (2012) 281–288.
[72] C. Jolicoeur, M.-A. Simard, Chemical admixture-cement interactions: phenomenology and physico-chemical concepts, Cem. Concr. Compos. 20 (2) (1998) 87–101.
[73] R.C. Kanning, K.F. Portella, M.O. Bragança, M.M. Bonato, J. dos Santos, Banana leaves ashes as pozzolan for concrete and mortar of Portland cement, Constr. Build. Mater. 54 (2014) 460–465.
[74] C. Karakurt, İ.B. Topçu, Effect of blended cements with natural zeolite and industrial by-products on rebar corrosion and high temperature resistance of concrete, Constr. Build. Mater. 35 (2012) 906–911.
[75] I. Kula, A. Olgun, V. Sevinc, Y. Erdogan, An investigation on the use of tincal ore waste, fly ash, and coal bottom ash as Portland cement replacement materials, Cem. Concr. Res. 32 (2) (2002) 227–232.
[76] H. Kurama, M. Kaya, Usage of coal combustion bottom ash in concrete mixture, Constr. Build. Mater. 22 (9) (2008) 1922–1928.
[77] K.-L. Lin, D.-F. Lin, W.-J. Wang, C.-C. Chang, T.-C. Lee, Pozzolanic reaction of a mortar made with cement and slag vitrified from a MSWI ash-mix and LED sludge, Constr. Build. Mater. 64 (2014) 277–287.
[78] K.L. Lin, C.L. Hwang, J.L. Shie, Y.M. Chang, A. Cheng, Hydration characteristics of waste catalysts used as pozzolanic materials, Environ. Prog. Sustain. Energy 33 (2) (2014) 353–358.
[79] M. Lorenzo, S. Goni, A. Guerrero, Role of aluminous component of fly ash on the durability of Portland cement-fly ash pastes in marine environment, Waste Manage. 23 (8) (2003) 785–792.
[80] M. Madani Hosseini, Y. Shao, J.K. Whalen, Biocement production from silicon-rich plant residues: perspectives and future potential in Canada, Biosyst. Eng. 110 (4) (2011) 351–362.
[81] Y. Maltais, J. Marchand, Influence of curing temperature on cement hydration and mechanical strength development of fly ash mortars, Cem. Concr. Res. 27 (7) (1997) 1009–1020.
[82] B.K. Marsh, R.L. Day, Pozzolanic and cementitious reactions of fly ash in blended cement pastes, Cem. Concr. Res. 18 (2) (1988) 301–310.
[83] C. Medina, P. Banfill, M. Sánchez de Rojas, M. Frías, Rheological and calorimetric behaviour of cements blended with containing ceramic sanitary ware and construction/demolition waste, Constr. Build. Mater. 40 (2013) 822–831.
[84] P.K. Mehta, Pozzolanic and Cementitious Byproducts as Mineral Admixtures for Concrete – A Critical Review, ACI Special Publication, 1983, p. 79.
[85] K. Montakarntiwong, N. Chusilp, W. Tangchirapat, C. Jaturapitakkul, Strength and heat evolution of concretes containing bagasse ash from thermal power plants in sugar industry, Mater. Design 49 (2013) 414–420.
[86] Y. Morozov, A. Castela, A. Dias, M. Montemor, Chloride-induced corrosion behavior of reinforcing steel in spent fluid cracking catalyst modified mortars, Cem. Concr. Res. 47 (2013) 1–7.
[87] D.G. Nair, A. Fraaij, A.A. Klaassen, A.P. Kentgens, A structural investigation relating to the pozzolanic activity of rice husk ashes, ***Cem. Concr. Res. 38 (6) (2008) 861–869.
[88] M. Narmluk, T. Nawa, Effect of curing temperature on pozzolanic reaction of fly ash in blended cement paste, Int. J. Chem. Eng. Appl. 5 (1) (2014) 31–35.
[89] R.-U.-D. Nassar, P. Soroushian, T. Ghebrab, Field investigation of high-volume fly ash pavement concrete, Resourc. Conserv. Recycl. 73 (2013) 78–85.
[90] M. Nehdi, J. Duquette, A. El Damatty, Performance of rice husk ash produced using a new technology as a mineral admixture in concrete, Cem. Concr. Res. 33 (8) (2003) 1203–1210.
[91] C. Ogden, K. Ileleji, K. Johnson, Q. Wang, In-field direct combustion fuel property changes of switchgrass harvested from summer to fall, Fuel Process. Technol. 91 (3) (2010) 266–271.
[92] H.M. Owaid, R. Hamid, M. Taha, Influence of thermally activated alum sludge ash on the engineering properties of multiple-blended binders concretes, Constr. Build. Mater. 61 (2014) 216–229.

[93] M. Pala, E. Özbay, A. Öztaş, M.I. Yuce, Appraisal of long-term effects of fly ash and silica fume on compressive strength of concrete by neural networks, Constr. Build. Mater. 21 (2) (2007) 384–394.
[94] S.-C. Pan, D.-H. Tseng, C.-C. Lee, C. Lee, Influence of the fineness of sewage sludge ash on the mortar properties, Cem. Concr. Res. 33 (11) (2003) 1749–1754.
[95] N. Panwar, S. Kaushik, S. Kothari, Role of renewable energy sources in environmental protection: a review, Renew. Sustain. Energy Rev. 15 (3) (2011) 1513–1524.
[96] V. Papadakis, S. Tsimas, Supplementary cementing materials in concrete: Part I: efficiency and design, Cem. Concr. Res. 32 (10) (2002) 1525–1532.
[97] V.G. Papadakis, Effect of fly ash on Portland cement systems: Part I. Low-calcium fly ash, Cem. Concr. Res. 29 (11) (1999) 1727–1736.
[98] R. Parichatprecha, P. Nimityongskul, Analysis of durability of high performance concrete using artificial neural networks, Constr. Build. Mater. 23 (2) (2009) 910–917.
[99] J. Payá, J. Monzó, M. Borrachero, Fluid catalytic cracking catalyst residue (FC3R): an excellent mineral by-product for improving early-strength development of cement mixtures, Cem. Concr. Res. 29 (11) (1999) 1773–1779.
[100] J. Payá, J. Monzo, M. Borrachero, E. Peris-Mora, F. Amahjour, Mechanical treatment of fly ashes: Part IV. Strength development of ground fly ash-cement mortars cured at different temperatures, Cem. Concr. Res. 30 (4) (2000) 543–551.
[101] J. Payá, J. Monzó, M. Borrachero, S. Velázquez, Cement equivalence factor evaluations for fluid catalytic cracking catalyst residue, Cem. Concr. Compos. 39 (2013) 12–17.
[102] J. Payá, J. Monzó, M. Borrachero, S. Velázquez, Evaluation of the pozzolanic activity of fluid catalytic cracking catalyst residue (FC3R). Thermogravimetric analysis studies on FC3R-Portland cement pastes, Cem. Concr. Res. 33 (4) (2003) 603–609.
[103] J. Payá, J.M. Monzó, M.V. Borrachero, S. Velázquez, Pozzolanic reaction rate of fluid catalytic cracking catalyst residue (FC3R) in cement pastes, Adv. Cem. Res. 25 (2) (2013) 112–118.
[104] C. Poon, X. Qiao, Z. Lin, Pozzolanic properties of reject fly ash in blended cement pastes, Cem. Concr. Res. 33 (11) (2003) 1857–1865.
[105] C.S. Poon, S.C. Kou, L. Lam, Z.S. Lin, Activation of fly ash/cement systems using calcium sulfate anhydrite (CaSO4), Cem. Concr. Res. 31 (6) (2001) 873–881.
[106] A. Pourkhorshidi, M. Najimi, T. Parhizkar, F. Jafarpour, B. Hillemeier, Applicability of the standard specifications of ASTM C618 for evaluation of natural pozzolans, Cem. Concr. Compos. 32 (10) (2010) 794–800.
[107] B. Prasad, H. Eskandari, B. Reddy, Prediction of compressive strength of SCC and HPC with high volume fly ash using ANN, Constr. Build. Mater. 23 (1) (2009) 117–128.
[108] R. Rajamma, R.J. Ball, L.A. Tarelho, G.C. Allen, J.A. Labrincha, V.M. Ferreira, Characterisation and use of biomass fly ash in cement-based materials, J. Hazard. Mater. 172 (2) (2009) 1049–1060.
[109] C. Rattanashotinunt, P. Thairit, W. Tangchirapat, C. Jaturapitakkul, Use of calcium carbide residue and bagasse ash mixtures as a new cementitious material in concrete, Mater. Design 46 (2013) 106–111.
[110] I. Richardson, The nature of CSH in hardened cements, Cem. Concr. Res. 29 (8) (1999) 1131–1147.
[111] G. Rodríguez de Sensale, Strength development of concrete with rice-husk ash, Cem. Concr. Compos. 28 (2) (2006) 158–160.
[112] M.F.A. Rojas, M.I. Sánchez de Rojas, The effect of high curing temperature on the reaction kinetics in MK/lime and MK-blended cement matrices at 60 °C, Cem. Concr. Res. 33 (5) (2003) 643–649.
[113] E. Rubio, V. Rodríguez, S. Alcocer, V. Castaño, Rice husks as source for pozzolan nanomaterials, Mater. Res. Innov. 15 (4) (2011) 268–270.
[114] S. Rukzon, P. Chindaprasirt, R. Mahachai, Effect of grinding on chemical and physical properties of rice husk ash, Int. J. Min. Met. Mater. 16 (2) (2009) 242–247.
[115] M.I. Sánchez de Rojas, M. Frías, O. Rodríguez, J. Rivera, Durability of blended cement pastes containing ceramic waste as a pozzolanic addition, J. Am. Ceram. Soc. 97 (5) (2014) 1543–1551.
[116] M. Sarıdemir, Prediction of compressive strength of concretes containing metakaolin and silica fume by artificial neural networks, Adv. Eng. Softw. 40 (5) (2009) 350–355.
[117] V. Sata, C. Jaturapitakkul, K. Kiattikomol, Influence of pozzolan from various by-product materials on mechanical properties of high-strength concrete, Constr. Build. Mater. 21 (7) (2007) 1589–1598.
[118] V. Sata, C. Jaturapitakkul, C. Rattanashotinunt, Compressive strength and heat evolution of concretes containing palm oil fuel ash, J. Mater. Civil Eng. 22 (10) (2010) 1033–1038.
[119] V. Sata, J. Tangpagasit, C. Jaturapitakkul, P. Chindaprasirt, Effect of W/B ratios on pozzolanic reaction of biomass ashes in Portland cement matrix, Cem. Concr. Compos. 34 (1) (2012) 94–100.
[120] Y. Shao, T. Lefort, S. Moras, D. Rodriguez, Studies on concrete containing ground waste glass, Cem. Concr. Res. 30 (1) (2000) 91–100.
[121] C. Shi, R.L. Day, Acceleration of strength gain of lime-pozzolan cements by thermal activation, Cem. Concr. Res. 23 (4) (1993) 824–832.
[122] C. Shi, R.L. Day, Comparison of different methods for enhancing reactivity of pozzolans, Cem. Concr. Res. 31 (5) (2001) 813–818.
[123] C. Shi, R.L. Day, Pozzolanic reaction in the presence of chemical activators: Part I. Reaction kinetics, Cem. Concr. Res. 30 (1) (2000) 51–58.
[124] C. Shi, R.L. Day, Pozzolanic reaction in the presence of chemical activators: Part II—Reaction products and mechanism, Cem. Concr. Res. 30 (4) (2000) 607–613.
[125] H.-S. Shi, L.-L. Kan, Leaching behavior of heavy metals from municipal solid wastes incineration (MSWI) fly ash used in concrete, J. Hazard. Mater. 164 (2) (2009) 750–754.
[126] R. Siddique, Performance characteristics of high-volume Class F fly ash concrete, Cem. Concr. Res. 34 (3) (2004) 487–493.
[127] N. Singh, S. Rai, Effect of polyvinyl alcohol on the hydration of cement with rice husk ash, Cem. Concr. Res. 31 (2) (2001) 239–243.
[128] T. Sinsiri, W. Kroehong, C. Jaturapitakkul, P. Chindaprasirt, Assessing the effect of biomass ashes with different finenesses on the compressive strength of blended cement paste, Mater. Design 42 (2012) 424–433.
[129] R. Somna, C. Jaturapitakkul, P. Rattanachu, W. Chalee, Effect of ground bagasse ash on mechanical and durability properties of recycled aggregate concrete, Mater. Design 36 (2012) 597–603.
[130] S. Swaddiwudhipong, H. Wu, M. Zhang, Numerical simulation of temperature rise of high strength concrete incorporating silica fume and superplasticiser, Adv. Cem. Res. 15 (4) (2003) 161–169.
[131] W. Tangchirapat, S. Khamklai, C. Jaturapitakkul, Use of ground palm oil fuel ash to improve strength, sulfate resistance, and water permeability of concrete containing high amount of recycled concrete aggregates, Mater. Design 41 (2012) 150–157.
[132] M. Thomas, The effect of supplementary cementing materials on alkali-silica reaction: a review, Cem. Concr. Res. 41 (12) (2011) 1224–1231.
[133] I.B. Topcu, M. Sarıdemir, Prediction of compressive strength of concrete containing fly ash using artificial neural networks and fuzzy logic, Comp. Mater. Sci. 41 (3) (2008) 305–311.
[134] C.-J. Tsai, R. Huang, W.-T. Lin, H.-N. Wang, Mechanical and cementitious characteristics of ground granulated blast furnace slag and basic oxygen furnace slag blended mortar, Mater. Design 60 (2014) 267–273.
[135] N. Ukrainczyk, E.A. Koenders, K.v. Breugel, Simulation of Pozzolan Blended cement hydration, in: Proceedings of the First International Conference on Concrete Sustainability, 2013, pp. 27–29.
[136] N. Van Tuan, G. Ye, K. Van Breugel, A.L. Fraaij, D.D. Bui, The study of using rice husk ash to produce ultra high performance concrete, Constr. Build. Mater. 25 (4) (2011) 2030–2035.
[137] V.-T.-A. Van, C. Rößler, D.-D. Bui, H.-M. Ludwig, Mesoporous structure and pozzolanic reactivity of rice husk ash in cementitious system, Constr. Build. Mater. 43 (2013) 208–216.
[138] S.V. Vassilev, C.G. Vassileva, A new approach for the classification of coal fly ashes based on their origin, composition, properties, and behaviour, Fuel 86 (10) (2007) 1490–1512.
[139] V. Vasugi, K. Ramamurthy, Identification of design parameters influencing manufacture and properties of cold-bonded pond ash aggregate, Mater. Design 54 (2014) 264–278.
[140] A.G. Vayghan, A. Khaloo, S. Nasiri, F. Rajabipour, Studies on the effect of retention time of rice husk combustion on the ash's chemo-physical properties and performance in cement mixtures, J. Mater. Civil Eng. 24 (6) (2011) 691–697.
[141] E. Villar-Cociña, E.V. Morales, S.F. Santos, H. Savastano Jr, M. Frías, Pozzolanic behavior of bamboo leaf ash: characterization and determination of the kinetic parameters, Cement Concrete Comp. 33 (1) (2011) 68–73.
[142] E. Villar-Cociña, E. Valencia-Morales, R. Gonzalez-Rodrıguez, J. Hernandez-Ruız, Kinetics of the pozzolanic reaction between lime and sugar cane straw ash by electrical conductivity measurement: a kinetic–diffusive model, Cem. Concr. Res. 33 (4) (2003) 517–524.
[143] S. Wang, L. Baxter, Comprehensive study of biomass fly ash in concrete: strength, microscopy, kinetics and durability, Fuel Process. Technol. 88 (11) (2007) 1165–1170.
[144] S. Wang, A. Miller, E. Llamazos, F. Fonseca, L. Baxter, Biomass fly ash in concrete: mixture proportioning and mechanical properties, Fuel 87 (3) (2008) 365–371.
[145] X.-Y. Wang, H.-S. Lee, K.-B. Park, Simulation of low-calcium fly ash blended cement hydration, ACI Mater. J. 106 (2) (2009).
[146] X. Wang, H. Lee, S.-W. Shin, J. Golden, Simulation of a temperature rise in concrete incorporating silica fume, Mag. Concrete Res. 62 (9) (2010) 637–646.
[147] Y. Wang, Y. Shao, M.D. Matovic, J.K. Whalen, Recycling of switchgrass combustion ash in cement: characteristics and pozzolanic activity with chemical accelerators, Constr. Build. Mater. 73 (2014) 472–478.
[148] S. Wansom, S. Janjaturaphan, S. Sinthupinyo, Characterizing pozzolanic activity of rice husk ash by impedance spectroscopy, Cem. Concr. Res. 40 (12) (2010) 1714–1722.
[149] I. Wilińska, B. Pacewska, Calorimetric and thermal analysis studies on the influence of waste aluminosilicate catalyst on the hydration of fly ash–cement paste, J. Therm. Anal. Calorim. 116 (2) (2014) 689–697.
[150] A. Williams, J. Jones, L. Ma, M. Pourkashanian, Pollutants from the combustion of solid biomass fuels, Prog. Energy Combust. 38 (2) (2012) 113–137.
[151] W. Xu, T.Y. Lo, S.A. Memon, Microstructure and reactivity of rich husk ash, Constr. Build. Mater. 29 (2012) 541–547.
[152] J. Yajun, J. Cahyadi, Simulation of silica fume blended cement hydration, Mater. Struct. 37 (6) (2004) 397–404.
[153] M.O. Yusuf, M.A. Megat Johari, Z.A. Ahmad, M. Maslehuddin, Strength and microstructure of alkali-activated binary blended binder containing palm oil

fuel ash and ground blast-furnace slag, Constr. Build. Mater. 52 (2014) 504–510.
[154] M. Zain, M. Islam, F. Mahmud, M. Jamil, Production of rice husk ash for use in concrete as a supplementary cementitious material, Constr. Build. Mater. 25 (2) (2011) 798–805.
[155] G. Zhang, B. Eddy Patuwo, Y. Hu, Forecasting with artificial neural networks: the state of the art, Inter. J. Forecasting 14 (1) (1998) 35–62.
[156] Y.M. Zhang, W. Sun, H.D. Yan, Hydration of high-volume fly ash cement pastes, Cem. Concr. Compos. 22 (6) (2000) 445–452.
[157] S. Zhou, X.A. Zhang, X. Chen, Pozzolanic activity of feedlot biomass (cattle manure) ash, Constr. Build. Mater. 28 (1) (2012) 493–498.
[158] E. Zornoza, P. Garcés, J. Monzó, M. Borrachero, J. Payá, Compatibility of fluid catalytic cracking catalyst residue (FC3R) with various types of cement, Adv. Cem. Res. 19 (3) (2007) 117–124.